POLITECNICO DI TORINO

Master's Degree in Electronic Engineering

Master's Degree Thesis

Blue energy harvesting: development of supercapacitor devices with CNT-based electrodes for CapMix applications

Supervisor

Prof. Andrea LAMBERTI

Dott. Alessandro PEDICO

Candidate

Yari BLANDOLINO

December 2023

Summary

Salinity Gradient Energy (SGE) is an alternative method to produce clean energy exploiting the difference of salinity of two fluids. In particular, Capacitive Mixing (CapMix) is a particular SGE technique that exploits two solutions (usually salt water and fresh water) which are alternatively injected in a cell. This technique can be very helpful to fulfill the increasing global energy demand and to become more independent from non renewable energy sources. Furthermore, CapMix devices can be very small and directly produce electrical energy without any conversion (usually from mechanical to electrical).

The aim of this thesis is to demonstrate that carbon nanotube-based tapes can be used as electrodes in a CapMix cell.

In chapter 1, a theoretical revision of SGP techniques is conducted. Also, a state of the art of this processes is presented.

In chapter 2, Capacitive Mixing is explained. The CapMix cycle is presented and it is shown how it is possible to harvest energy from this process.

In chapter 3, the supercapacitor is presented, which is the energy storage device exploited in CapMix. Also, the most used carbon-based electrodes are discussed, including CNTs.

In chapter 4, the principal evaluation techniques are explained. Furthermore, the most critical parameter for the CapMix study are presented.

In chapter 5, carbon nanotubes are studied. Electrochemical characterizations and electrical measurements are conducted on these single electrodes to evaluate their performance in NaCl solution and also in brine.

In chapter 6, CapMix measurements are done using the CNT electrodes. First of all, a specific cell is designed and produced for this case, and then the SGP process

is performed using this device and the electrodes.

In chapter 7, a final recap is done on the obtained results and some suggestions for future research are given.

Acknowledgements

"Un sentito ringraziamento al prof. Andrea Lamberti e ad Alessandro Pedico per la loro disponibilità e cordialità, e per avermi accompagnato in questo percorso di tesi con preziosi consigli ed insegnamenti.

Ringrazio la mia famiglia per avermi supportato moralmente ed economicamente, e per essermi sempre stata vicina anche quando fisicamente distante.

Ringrazio i miei amici di sempre per i bei momenti passati insieme, che mi hanno fatto ricordare che anche un ingegnere può divertirsi ogni tanto.

Infine, ringrazio i miei compagni di università e i numerosi coinquilini per aver condiviso le difficoltà e le gioie di questo percorso universitario."

Yari

Table of Contents

List of Tables

List of Figures

Acronyms

AC

Activated Carbon

AccMix

Accumulator Mixing

AEM

Anionic-selective membranes

CapMix

Capacitive Mixing

CCCD

Constant Current Charge/Discharge

CEM

Cationic-selective Membranes

CNT

Carbon Nanotube

CP

Chronopotentiometry

CV

Cyclic Voltammetry

DW-CNT

Double walled Carbon Nanotube

EDL

Electrical Double Layer

EDLC

Electrical Double Layer Capacitor

EIS

Electrochemical Impedance Spectroscopy

ESR

Equivalent Series Resistance

IHP

Inner Helmholtz Plane

MW-CNT

Multi walled Carbon Nanotube

OHP

Outer Helmholtz Plane

OCP

Open Circuit Potential

PC

Pseudocapacitor

PEIS

Potentiostatic Electrochemical Impedance Spectroscopy

PMMA

Polymethyl methacrylate

RED

Reverse ElectroDialysis

redox

oxidation-reduction

SC

Supercapacitor

SGE

Salinity Gradient Energy

SGP

Salinity Gradient Power

SW-CNT

Single walled Carbon Nanotube

Chapter 1

Salinity Gradient Power

In recent years, the world population growth (8.5 billions in 2030, 9.7 billions in 2050 and 10.4 billions in 2100 [1]) has led to an increase of food, water and electricity demand. In order to fulfill this necessity, new energy sources must be found since traditional source energies (oil, natural gas, coal, etc...) won't be a sustainable contribution. Therefore, renewable sources like solar, wind and biomass must be chosen.
Several studies have been done by researchers to find new energy sources. A field of this research concerns the so called 'Blue Energy', which is referred to all the types of techniques that are able to harvest energy from the sea and water in general. A particular example is the Salinity Gradient Energy (SGE) or Salinity Gradient Power (SGP), which can be obtained when two solutions with different salinity gradients mix together: this happens when a river flows into the sea and results in a dissipation of free energy. In order to harvest this energy, a controlled mixing of the two solutions (sea water and river water) must be performed by a suitable device; in this way, the free dissipated energy is not lost but it is recovered and can be employed for human necessities. This is a completely green energy source, since it is renewable and does not produce any carbon products; it also solves the other green sources problems, since power production is continuous (while solar and wind, for example, suffer from production's discontinuity). A rough estimate of world theoretical potential of SGP regarding rivers flowing into the sea goes from 1.4 to 2.7 TW [2]. The real potential (0.2 to 1 TW [2]) is only a fraction of the theoretical one since process efficiencies and practicabilities limit the harvesting operation.

1.1 State of the Art

SGP technologies can be divided and organized according to several criteria. For example, an initial classification can be done looking at the type of process (figure 1.1).

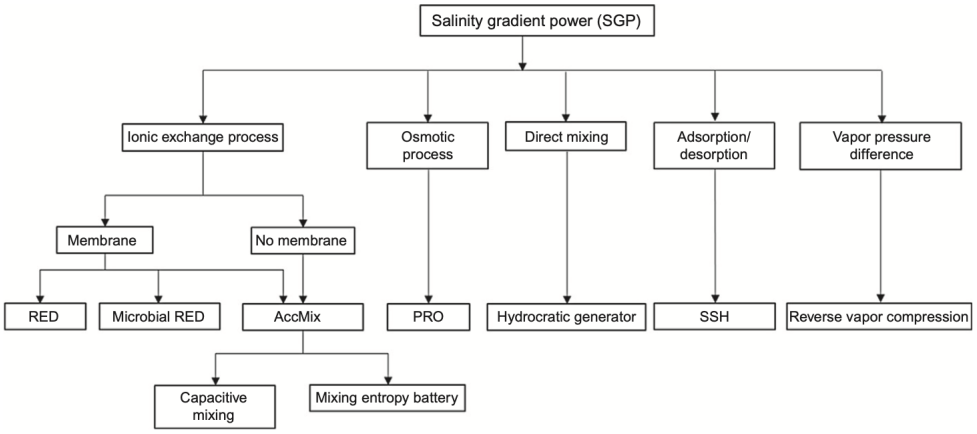

Figure 1.1: SGP: classification based on the type of process [3]

Five different processes can be identified with this schematic:

A. **Ionic exchange process:** a change of concentration of the two solutions depends on ions transport (anions and cations). This technique can use either membranes or not.
Reverse ElectroDialysis (RED) exploits ionic exchange membranes to achieve a controlled mixing of the two solutions [4]. In particular, cationic-selective membranes (CEM) and anionic-selective membranes (AEM) are placed in a stack where the solutions are forced to flow, driven by concentration gradients. This ionic flux, regulated by the membranes, is converted into an electric current through redox reactions at the extremities of the stack. In this way, a voltage variation can be observed.
Accumulator Mixing (AccMix) is a technique that can be used with or without membranes. It consists of a four-step cycle where the two electrodes accumulate charge in the high salinity solution and release it in the low salinity solution. This leads to a net energy production since the charge accumulated on the electrodes is lower than the charge released during the discharging step [5]. More details on this technique will be given in the following sections.

B. **Osmotic processes:** they refer to a kind of process where the solvent (water, etc...) causes the concentration change in the solutions.

In *Pressure Retarded Osmosis* (PRO) the two solutions are separated by an osmotic membrane. The solvent passes through this membrane causing a variation of the chemical potential of the solutions. The water flow can be retarded by a hydrostatic pressure [6].

C. **Direct mixing:** it is a technique where both the solvent and the ions are moving, and the two solutions are mixed together. The *Hydrocratic Generator* (HG) is an example of device that exploits this process [7]. A vertical tube is immersed in salt water, while fresh water is inserted by an inlet; this insertion causes an emission of both liquids while they mix together. A part of the energy needed to generate this flow comes directly from SGE and can be converted in mechanical work.

D. **Adsorption/desorption:** a particular material is used to adsorb the ions from the high salinity solution and desorb it in the low salinity one. *Swelling and Shrinking of Hydrogels* (SSH) is a new technology that makes use of polymeric hydrogels [8]. These hydrogels swell when they are in contact with fresh water and shrink when they are in contact with salt water due to adsorbtion/desorption. The SGE is captured and converted in potential energy if a weight is put on top of the hydrogel.

E. **Vapour pressure difference**: it exploits the vapour pressure difference between the two solutions. *Reverse Vapour Compression* (RVC) makes two liquids at different salinities evaporate. The higher pressure vapour (generated from low salinity solution) goes toward the other vapour (generated at lower pressure values). A turbine is able to recover this energy if it is put between the two chambers [9].

SGP techniques can be also classified depending on the type of energy produced. In fact, some of this processes directly convert electrochemical energy into electric energy, while some of them produce mechanical energy, which must be then converted in electrical energy. The latter option is usually less efficient since a further conversion means more dissipated energy and the process will last longer. In figure 1.2 this new sorting can be visualized.

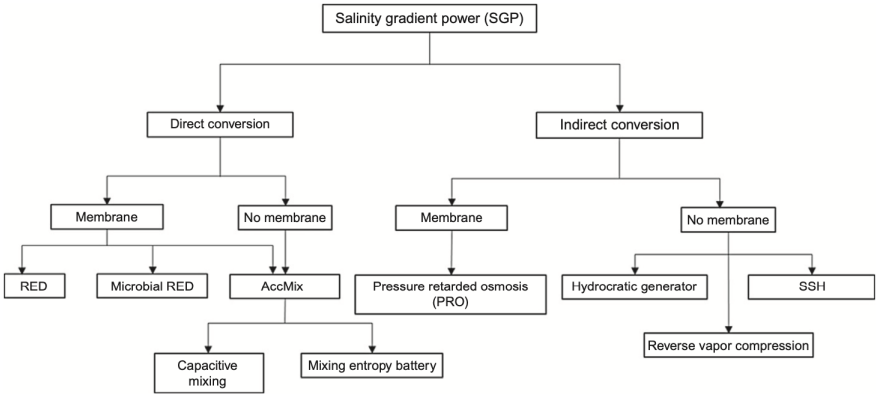

Figure 1.2: SGP: classification based on energy conversion [3]

A. **Direct conversion:** the electrical energy is produced in a single step, making it more efficient and rapid. RED and AccMix (which are based on ionic exchange) belong to this group.

B. **Indirect conversion:** these processes produce mechanical or potential energy which must be converted in electrical energy by a mechanical unit and an electrical generator, making the device more complex and less compact. Osmotic processes, direct mixing, adsorption/desorption, and vapour pressure difference belong to this group.

A further classification can be obtained separating the processes on the basis of the transported component (water or salt). Figure 1.3 highlights three main categories:

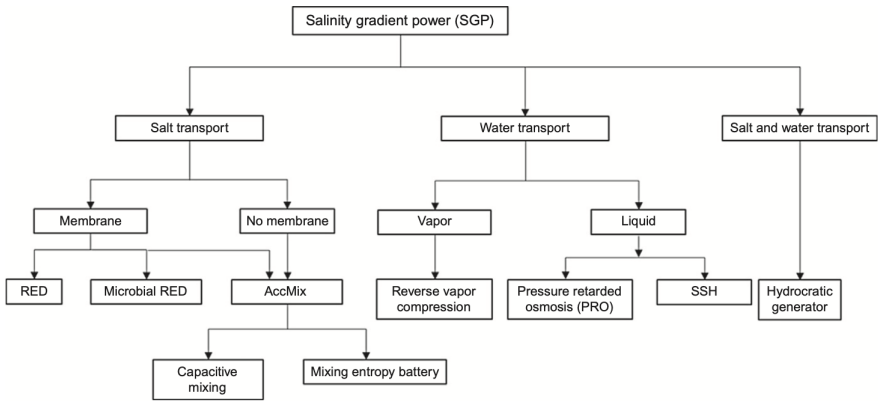

Figure 1.3: SGP: classification based on the transported species [3]

A. **Salt transport:** this category includes all the ionic exchange processes (RED, AccMix, ecc...).

B. **Water transport:** water can be transported in liquid phase (Pressure retarded osmosis, adsorpion/desorption) or vapour phase (Vapour pressure difference).

C. **Salt and water transport:** it is the case of direct mixing, where both ions and solutions are transported and mixed together.

Chapter 2

Capacitive Mixing

Capacitive Mixing is a technique based on electric double-layer (EDL) capacitors [5]. Two porous electrodes (usually made of carbon based materials) are put in contact with a liquid solution, creating a capacitor. When the capacitor is immersed in high salinity solution, charges are stored in the EDL (more on 3.4). When the high salinity solution is replaced by a low salinity solution, ions move away by diffusion and the voltage between plates increases. This process induces a surplus of electrostatic energy (at the expense of free energy of the two solutions) which can be harvested from the capacitor and converted in available power. Furthermore, the steps of this method are cyclic, so the energy extraction can be achieved by repeatedly operating the same procedure.

In this chapter, the CapMix process is presented. First of all, a general description of the four steps of this technique is done. After that, it is explained how it is possible to harvest new energy by looking at some critical parameters (voltage, charge, etc...). Finally, some drawbacks are taken into account and an alternative way to overcome these limits are proposed.

2.1 CapMix Cycle

The CapMix process can be split in four principal steps which can be cyclically repeated. A graphical representation of the cycle is presented in figure 2.1.

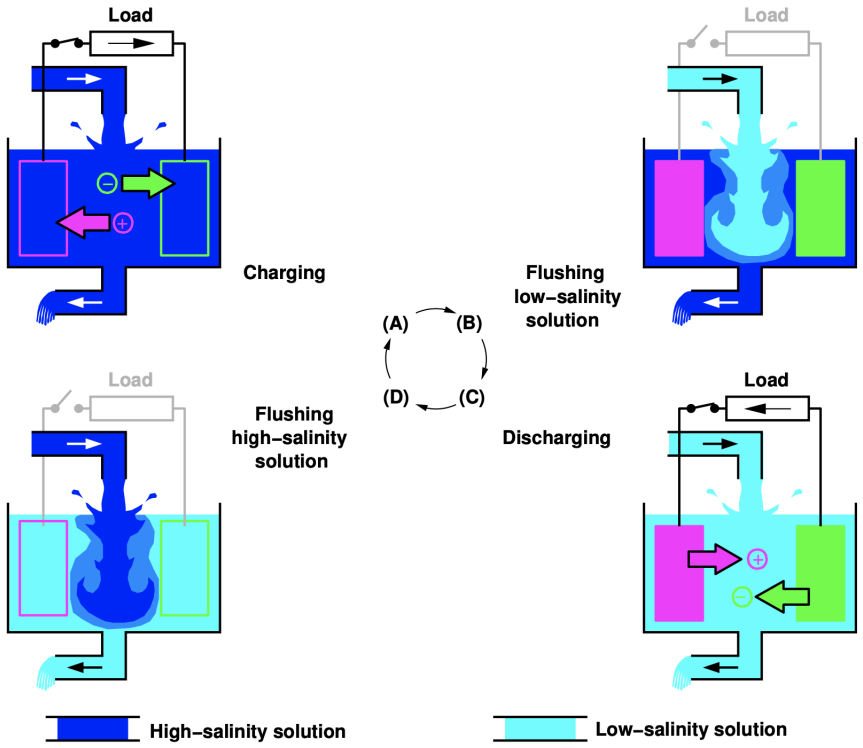

Figure 2.1: Schematic presentation of the CapMix cycle. [5]

A. The cell is filled with a high salinity solution. A current flows in the capacitor and each electrode repels ions of the same charge, while it attracts ions of opposite charge, forming an oppositely charged layer close to its surface [5]. Charge is therefore stored in the EDLs near the electrodes.

B. The circuit is opened and the high salinity solution is replaced by a low salinity solution.

C. Due to the ions discharging the electrodes (driven by diffusion), a current flows in the device but in the opposite direction with respect to the one in step A.

D. The circuit is opened again and the low salinity solution is replaced by the high salinity solution, making it possible to restart the cycle.

It is important to say that no electron moves between the electrodes and the solution since the device is operated with a voltage lower than the electrolytic potential of the ions in the solution [5]. In particular, this voltage is about 1 V for water solutions; if voltages higher than 1 V are applied, then a current will flow in the solution since redox chemical reaction will occur, discharging the EDLs.
The accumulation of ions in step A and the discharging in step C produce a net energy ΔG that is dissipated by the system. This loss of mixing free energy is dependent on the initial and final salt concentrations in the two solutions [3] and can be approximated by the formula:

$$\Delta G = RT\Delta n log\left(\frac{c_1^I}{c_2^I}\right) \tag{2.1}$$

where ΔG is actually the thermodynamically available free energy that can be transformed into electrical work [5]. In equation 2.1 R is the gas constant, T is the temperature, Δn is the vanishing transferred number of moles of salt, and finally c_1^I and c_2^I are respectively the initial concentration of the high-salinity (subscript 1) and low-salinity solutions (subscript 2).

2.2 Energy Harvesting

Energy extraction during the CapMix process can be possible: to demonstrate that, an analysis of some critical parameters (voltage, current, charge) is performed and discussed.
Figure 2.2 (from [3]) shows voltage and current values measured in the cell during all the CapMix steps.

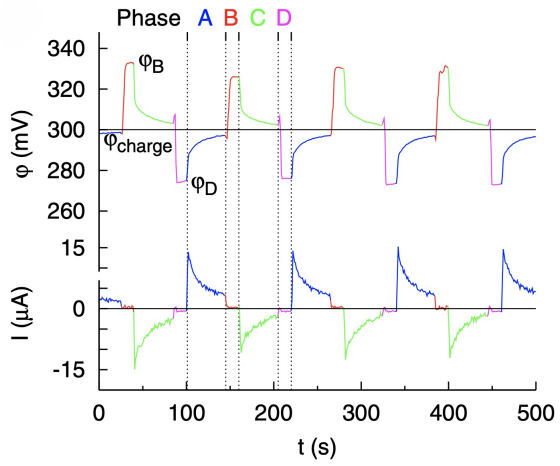

Figure 2.2: Voltage and current VS time during the CapMix cycle [3]

The cell voltage increases when the device is charged , while decreases when the cell is discharged. The charging step happens when the high salinity solution fills the cell, while the discharging step occurs when the low salinity solution is present in the device. Also, a voltage variation occurs both in steps B and D, corresponding to the open circuit states; this is due to the fact that two solutions with different ions concentration are mixed and this causes a variation of the chemical potential of the ions [3].
Figure 2.3 shows instead the voltage variation of the cell with respect to the stored charge.

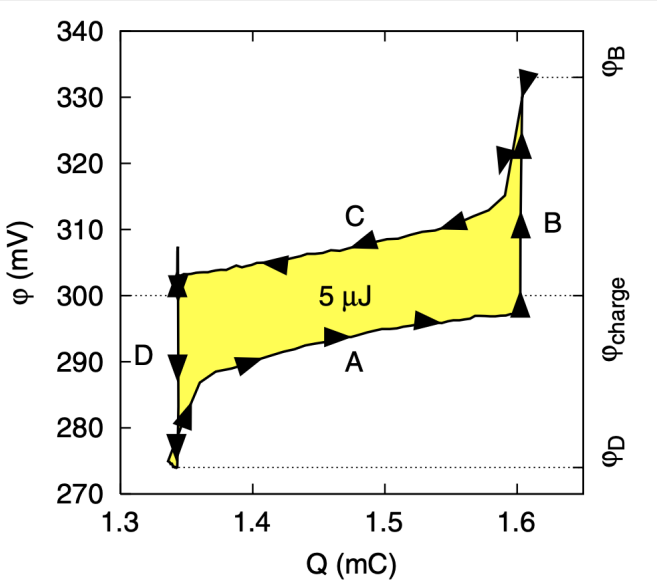

Figure 2.3: Voltage VS charge during the CapMix cycle [5]

The electrical work produced by the cell corresponds to the surface enclosed counterclockwise by the cycle (yellow area). The CapMix cycle actually follows this direction thanks to the voltage variation ΔV observed in figures 2.2 and 2.3, therefore an approximation of the work delivered by the cell can be obtained [3]:

$$W = \oint V(q)dq \approx \Delta V Q \tag{2.2}$$

where ΔV is the voltage variation (also called voltage rise) and Q is the charge exchanged per cycle.
The actual value of the energy produced in an AccMix cycle is known from 2.1, thus by equating $\Delta G = W$ it is found [3]:

$$\Delta V = \eta \frac{2RT}{F} log\left(\frac{c_1^I}{c_2^I}\right) \tag{2.3}$$

where $\eta = (e\Delta n)/Q$ is the so called "desalination charge efficiency", i.e. the number of moles of salt captured by the passage of one mole of charges through electrodes [3]. If $\eta = 1$ the case for ideal solutions is obtained, described by the Nerst law:

$$\Delta V = \frac{2RT}{F} log\left(\frac{c_1^I}{c_2^I}\right) \tag{2.4}$$

Equation 2.4 dictates a thermodynamic limit for all materials. According to the type of material utilized and to the polarity of the measurements, the cell voltage can be always positive, always negative or it can be positive for some steps and negative for the other ones. These three cases are reported in figure 2.4:

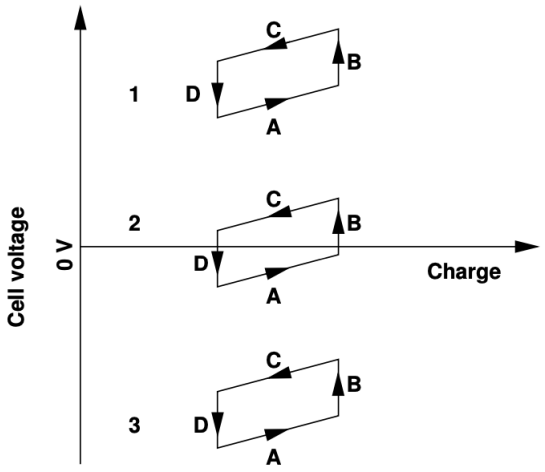

Figure 2.4: CapMix cycle for three different cases of voltage values. (1) Voltage always positive. (2) Voltage both positive and negative. (3) Voltage always negative [3]

In all three cases, an active step (discharge) and a passive step (charge) can be identified. The active step produces more energy than the passive one, therefore a net amount of energy is obtained.

2.2.1 Leakage Current and Spontaneous Potential

In an ideal scenario, the charge that is stored in phase A of the CapMix cycle (figure 2.1) should be the same amount of charge that is released in phase C. In

reality, the electrodes release less charge than what was taken due to the so called "leakage current" [10]. This means that the external power supply must replace the charge that is not available anymore. Furthermore, the power loss that is caused by the leakage current can be higher than the power produced by the CapMix technique, so no net power production is actually achieved. The reason behind the leakage is that carbon based electrodes are not ideally polarizable: they can be charged and maintain that charge for some minutes, but then they tend to move toward a specific spontaneous potential. From a chemical point of view, leakage consists in a recombination of charges inside the EDL (therefore redox reactions) leading to an overall reduction of the total charge accumulated in the EDL of one or both electrodes [10].

Figure 2.5 shows the effect of leakage on the energy extraction after some cycles:

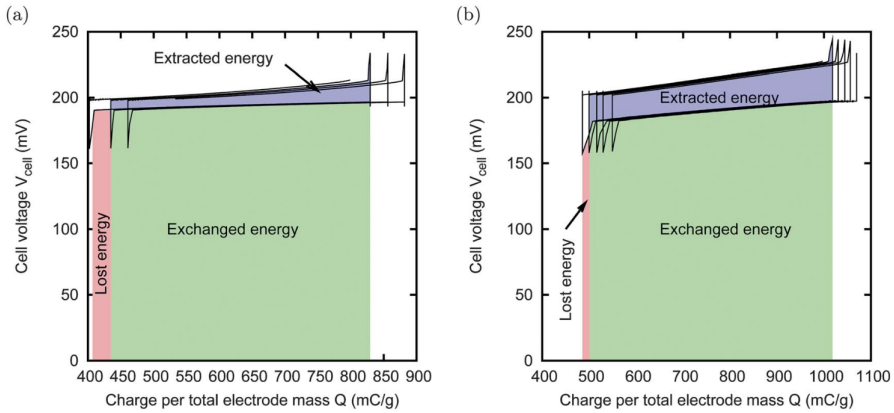

Figure 2.5: CapMix cycles with external voltage $V_{ext} = 200mV$ and concentrations $c_s = 500mM$ and $c_f = 20mM$. (a) THM sample, $R_{load,salt} = 5\Omega$, $R_{load,fresh} = 30\Omega$. (b) NS30, 45 mm thick film, $R_{load,salt} = 20\Omega$, $R_{load,fresh} = 90\Omega$. In both cases the electrode size is 15x15 mm, and the gap between them is 1 mm [10]

The area that lies under the curves (red and green regions) corresponds to the energy that is consumed by the electrical system, including the load and the power supply. The area that comprehends blue and green regions corresponds to the energy that is extracted from the cell. Therefore, since the green area is common to both cases, only the blue region describes a net energy production, while the red one is associated to energy loss. In fact, leakage current causes a drift towards right of the CapMix curves; without it, ideally no energy is lost.

This phenomenon is studied independently for singular electrodes, as shown in figure 2.6 [10].

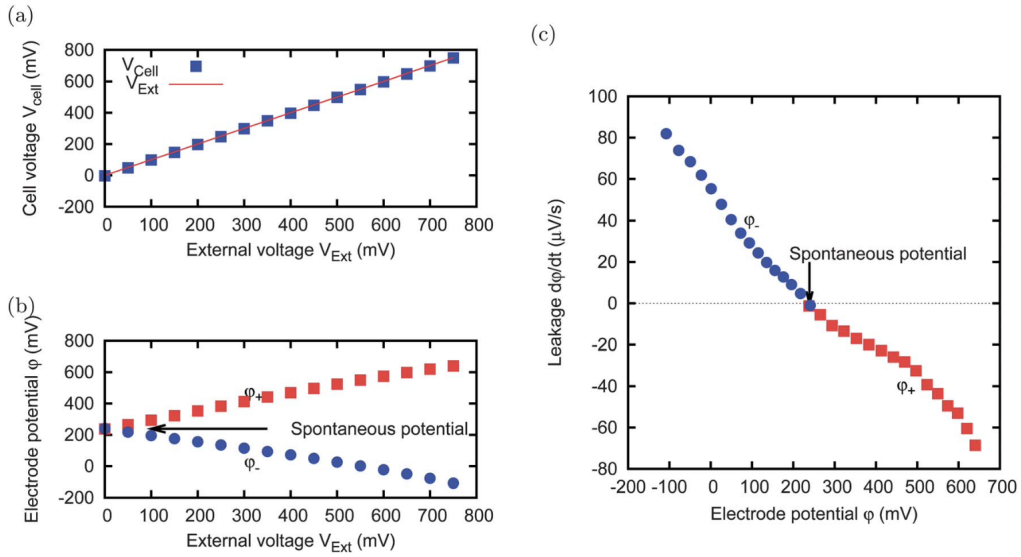

Figure 2.6: A cell with two electrodes is immersed in a $c_s = 500mM$ salt solution and charged for 10 minutes at several values of external voltage V_{ext} (shown in horizontal axis of (a) and (b)); then the circuit is opened for 30 seconds. [10]. (a) Cell voltage VS external voltage (b) Electrode potential VS external voltage (c) Leakage (potential fall speed) VS electrode potential [10]

An external voltage is applied at specific values for 10 minutes. From 2.6(b), when no external voltage is applied - so the cell is discharged - the electrodes are at the same potential which correspond to the previously discussed spontaneous potential. After every charging phase, the circuit is opened and the potential variation of each electrode is monitored. By looking at 2.6(c) it is found that the potential variation is zero when the electrodes are at the spontaneous potential; otherwise, leakage current will cause a potential fall that will drift those values towards the spontaneous potential. The more the potential of the electrode is distant from the spontaneous one, the stronger will be the leakage.
Obviously the voltage rise observed in a CapMix cycle is the contribution of the singular potential variation of both electrodes. Figure 2.7 shows the variation of the electrodes potentials (ϕ_+ and ϕ_-) due to concentration changes in the cell [10].

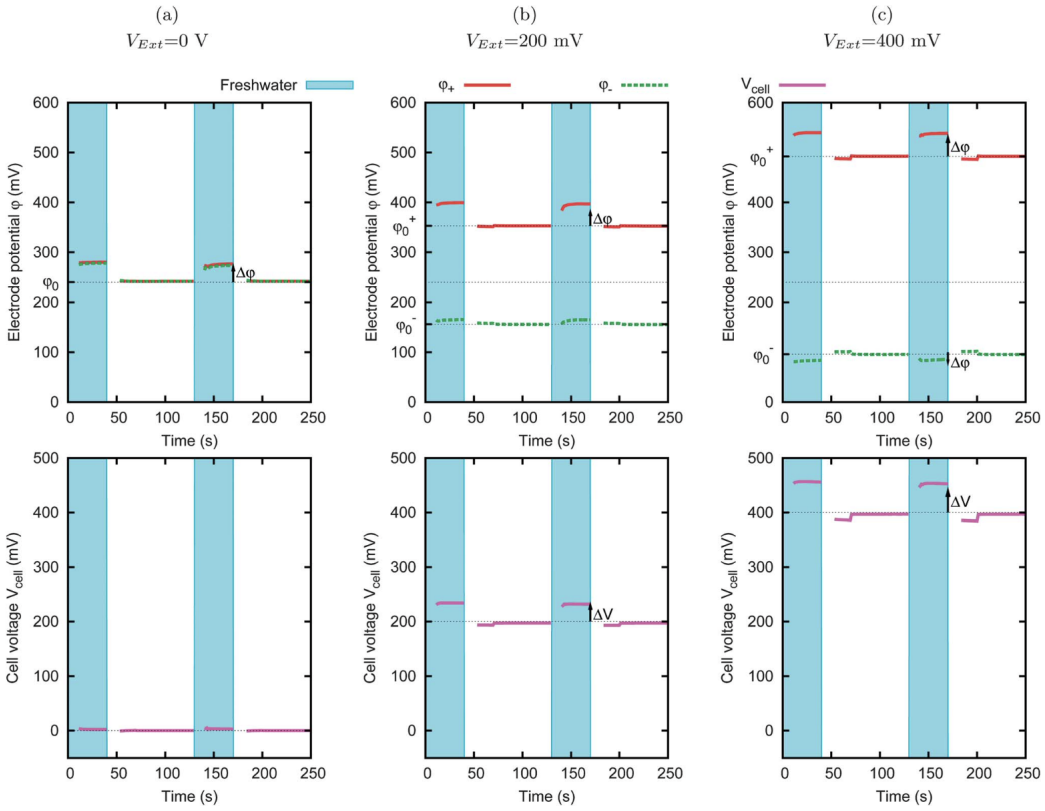

Figure 2.7: Effect of salinity change on the electrode potentials [10]

It is identified a base potential ϕ_0, which is the electrode potential in saltwater; the potential rise $\Delta\phi$ is the difference between the potential reached in freshwater and the base potential. In 2.7(a) the result is obtained for a discharged cell (V_{ext} = 0 V), while for 2.7(b) and 2.7(c) the cell is charged with an external voltage V_{ext}, meaning that the electrodes base voltage will be $\pm V_{ext}$ and the cell voltage will be $V_{cell} = V_{ext}$. When the solution is changed, a potential variation $\Delta\phi$ is observed for both electrodes for each value of V_{ext}. In particular, this phenomenon occurs also for case (a), i.e. when $V_{ext} = 0$ V; anyway, this effect can be observed only when the single potential of the electrodes are measured. In fact, the overall cell voltage is not affected by the concentration change.
However, it is known that the spontaneous potential differs from each material [10]. Therefore, if two electrodes with different materials are tested in a salt solution, two different spontaneous potentials and two different potential rises can be observed (figure 2.8). Also, the polarity of these potential variations can be opposite like in the case of the figure below.

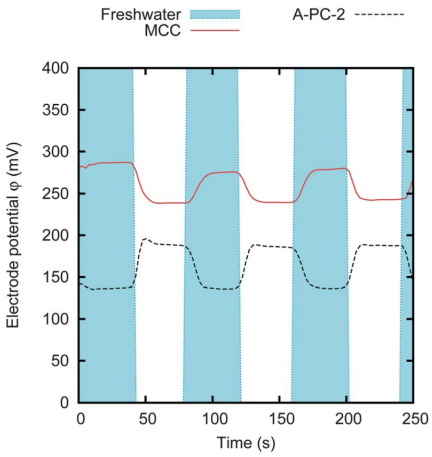

Figure 2.8: Potential variation upon salinity change, obtained without external charging ($V_{ext} = 0V$) for two different materials (MCC and A-PC-2) [10]

It is evident that using different materials for the positive and negative electrodes an improvement of the CapMix technique can be obtained. This knowledge can be exploited in two ways.
In the first case, two electrodes with different spontaneous potential and same potential rise can be chosen. The external voltage will be set to $V_{ext} = \Delta V_{spontaneous}$, where $\Delta V_{spontaneous}$ is the spontaneous voltage of the cell. In this way, no leakage would be observed since it takes the potential of the electrodes back to the spontaneous potential, but it doesn't happen. An example can be observed in figure 2.9 from [10].

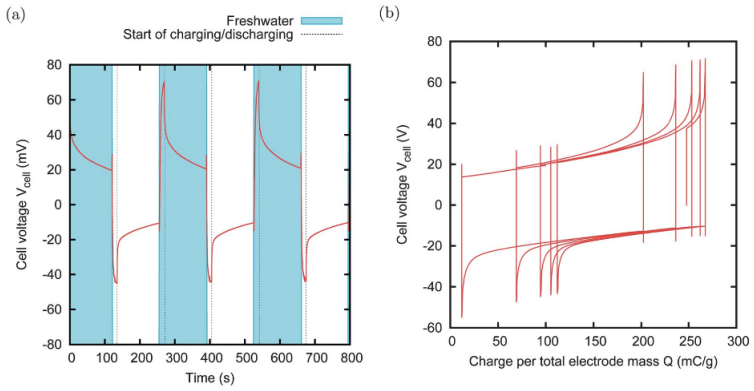

Figure 2.9: CapMix cycles with MCC and PAN [10]

In the second case, portrayed in figure 2.10 from [10], two electrodes with same

spontaneous potential but very different potential rises are chosen. The external voltage is set to zero but a voltage rise occurs anyway thanks to the extremely different potential rises. Another great advantage is that there is no leakage. This technique is called "zero charging" CapMix.

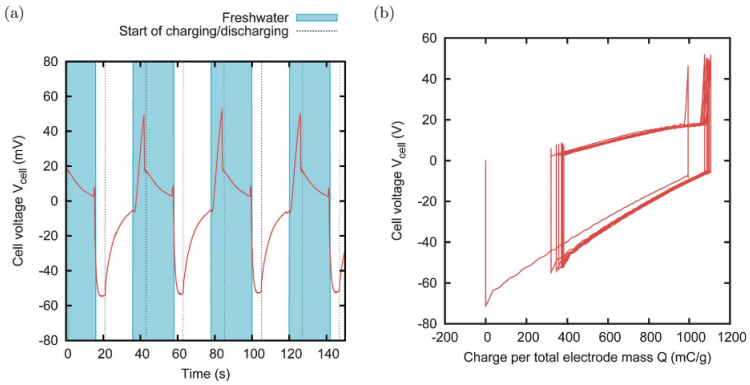

Figure 2.10: CapMix cycles with A-PC-2 and NS30 [10]

Chapter 3

Devices and Materials

3.1 Supercapacitors

Supercapacitors are energy storing devices that were recently developed to overcome several limitations of the common energy storage devices (batteries, capacitors, ecc...). They are able to collect a higher amount of energy density with respect to dielectric capacitors, and they deliver much more power density than batteries. Figure 3.1 shows the so called Ragone plot: it is a comparison of the main electrical energy storage devices by energy and power density.

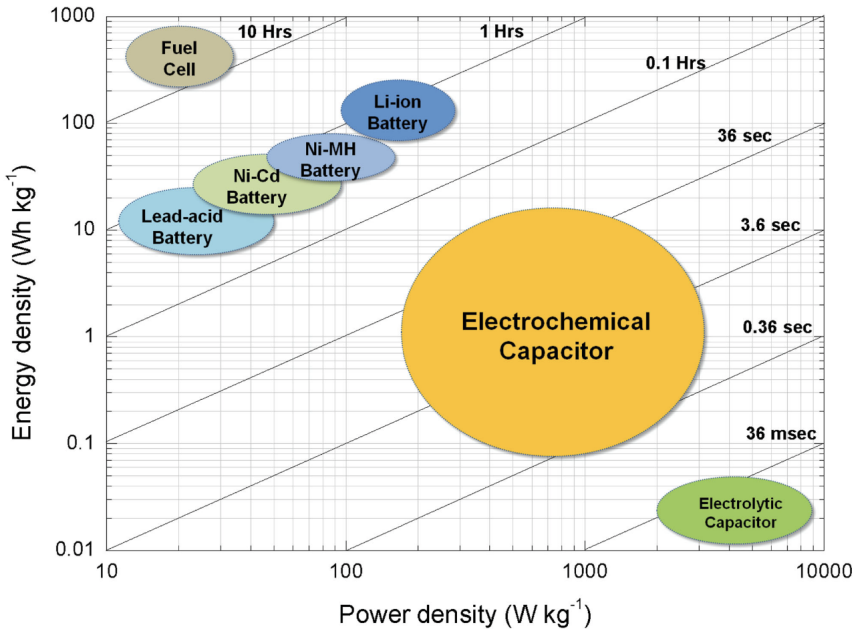

Figure 3.1: Ragone plot of energy storage devices [11]

Fuel cells are the ones with the most energy density available, followed by batteries which have also a better power density with respect to the very low value for fuel cells. Electrolytic capacitors are able to deliver a very high power density, but they can store a really low amount of energy. Supercapacitors, instead, show a very optimal performance in both cases, since they have a higher power density than fuel cells and batteries, and a higher energy density than electrolytic capacitors.

A typical supercapacitor cell is made up of two electrodes, an electrolyte and a separator. Usually, very high surface area electrodes and a small separation between them are chosen, in order to have a better capability to store a large amount of charge [12]. Although SCs have a higher power density and a better life cycle, they exhibit a low amount of energy stored per unit weight, higher dielectric adsorption and a faster self-discharge than batteries. Furthermore, if high voltages are applied to these devices, they suffer from corrosion or degradation [12]. Depending on the materials used for the electrodes and on the mechanism that allow to store charge, three types of supercapacitors exist:

1. Electric Double Layer Capacitors (EDLCs)

2. Pseudocapacitors (PCs)

3. Hybrid capacitors

3.1.1 EDLC: Electric Double Layer Capacitors

Electrical Double Layer Capacitors are able to store energy thanks to the formation of a double layer of charge at the surface between the electrodes and the electrolyte. The electrical double layer (EDL) that generates in these SCs was first described by Helmholtz. He modelled the interface between the electrolyte and the substrate as a capacitor (figure 3.2). From this description, the term "electrical double layer" was born, and then used also for the other models. The theory Helmholtz has developed was not accurate enough since a perfect layering of the charges cannot be possible due to thermal energy of the electrolyte solution.

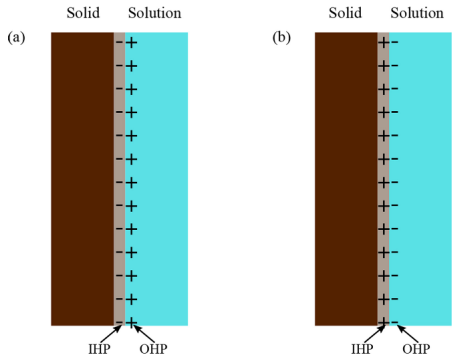

Figure 3.2: Helmholtz model of a charged interface between a solid dielectric substrate and an electrolyte solution [13]. (a) Negatively charged interface. (b) Positively charged interface. Arrows show inner Helmholtz plane (IHP) and outer Helmholtz plane (OHP).

Gouy-Chapman-Stern theory models the ion distribution close to planar electrodes as the sum of an adsorbed EDL (called Stern EDL), which contains only counterions, and a diffuse EDL that contain both coions and counterions but with a net excess charge [5]. The shear plane is at the interface between the two layers and its electrical potential is called zeta potential ζ [14]. Figure 3.3 presents a sketch of this model for two electrodes immersed in an electrolyte.

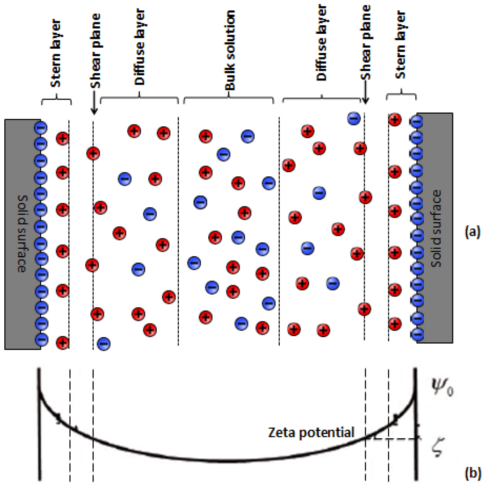

Figure 3.3: Schematic view of the EDL model. (a) Charge distribution. (b) Electric potential distribution. [14]

Charges accumulate in the diffuse EDL until an equilibrium between diffusion and

electrostatic force is reached. The former tends to equalize the charge distribution in the solution, while the latter tends to do the opposite by accumulated the charge close to the surface. This equilibrium state is described by the Poisson-Boltzmann equation; from this, a solution for ion concentrations and potential is obtained by Gouy and Chapman. In this configuration, the electric field is only present between the charge layers.

The relation between the surface charge density σ and the potential difference ϕ between the electrode and the bulk solution is:

$$\phi = \frac{2K_BT}{e} sinh^{-1}\left(\frac{\sigma}{\sqrt{8CN_A\epsilon_0\epsilon_rK_BT}}\right) \tag{3.1}$$

where K_B is the Boltzmann constant, T is the temperature, e is the electron charge, N_A is the Avogadro constant, ϵ_0 is the electric constant, ϵ_r is the relative dielectric constant, and C is the concentration [5]. The equation is valid for a symmetric, monovalent electrolyte as NaCl and shows that if the concentration decreases, then the potential increases. Equation 2.1 can be rewritten in terms of EDL effective thickness L, so that $\phi = \frac{L\sigma}{\epsilon_0\epsilon_r}$:

$$L = \lambda_S sinh^{-1}\left(\sqrt{\frac{\chi}{C}}\right) \tag{3.2}$$

where $\lambda_S = 2K_BT\epsilon_0\epsilon_r/(e\sigma)$ and $\chi = \sigma^2/(8N_A\epsilon_0\epsilon_rK_BT)$ [5].
In low concentration solutions the EDL has a bigger thickness, so the electric field can extend across a large portion of the solution because ions tend to move away from the electrode surface driven by diffusion. For high concentration solutions, the EDL becomes more thin since the ions move towards the surface of the electrode driven by the electrostatic forces.
If the electrode has pores, the model becomes more complex. If the pores have diameter much bigger than L, equation (1) holds. Otherwise, the pores are too small to contain the diffuse EDL so the capacity is lower with respect to the planar case [5].

3.1.2 Pseudocapacitors

Pseudocapacitors are based on rapid and reversible faradaic or redox reactions which occur near or at the electrodes surface [12]. There are three types of electrochemical mechanism that contribute to the energy storage:

- adsorption/desorption of protons or metal ions from the electrolyte
- redox reactions between electrode and electrolyte that cause charge transfer
- doping/undoping of an active material

The first two processes occur at the surface, while the third one is a bulk process. Anyhow, a suitable porous material is preferred for the electrode since it allows a better transfer of ions at the interface. A pseudocapacitive material can be extrinsic or intrinsic; an extrinsic material presents pseudocapacitive behaviour only when it has a nanoscale size, while an intrinsic material is pseudocapacitive for any type of size and geometry [12]. The most used materials for these devices are conductive polymers and metal oxides. Pseudocapacitors charge and discharge very quickly thanks to the rapid redox reactions, so they have high energy and power density. However, they present lower durability than EDLCs due to the same processes that degradate the electrodes material. The expression of the capacitance can be obtained by the derivative dq/dV, where dq is the charge variation and dV is the potential change [12].

3.1.3 Hybrid Supercapacitors

A hybrid supercapacitor is a supercapacitor that exploits both EDL and faradaic redox reactions. It is formed by a cathode and an anode made of different active materials, a separator, and alectrolyte. By exploiting both electrical double layer and faradaic redox reactions, higher energy and power density can be achieved. Also EDL electrode contributes to a much better reliability and durability, since the electrode material is not ruined by continuous chemical reactions at its surface [12].

3.2 Electrodes

It has been found that carbon-based materials are well suited for EDLC applications. They are very diffused because they are really cheap, easy to obtain and very durable. When they are used as electrodes in a SC cell, they are able to store charge thanks to the EDLs that form at the interface between the electrolyte and electrodes. The capacitance associated to the double layer can be assumed to be:

$$C = \frac{A\epsilon}{4\pi d} \tag{3.3}$$

where A is the area of the electrode, ϵ is the dielectric constant of the electrolyte and d is the thickness of the double layer [15]. Therefore, to improve the storage capacity, porous structures with large surface areas are needed, in order to assure a suitable charge transport. The ion transport can be described with equation 3.4:

$$\tau = \frac{L^2}{D} \tag{3.4}$$

where L is the ion transport length and D is the ion transport coefficient [15]. Nanomaterials, which can be derived from carbon precursors, exhibit a better performance since the ion transport length (L) is much more smaller than other materials.

For CapMix applications, usually four types of electrode structures are exploited:

(a) Electrode charged with external voltage supply

(b) Charged adsorbed molecules on the electrode surface

(c) Electrode with surface coated by charged polymers

(d) Ion-exchange membranes (composed by charged molecules) covering the electrodes

In figure 3.4, the charge distribution of these four applications are presented.

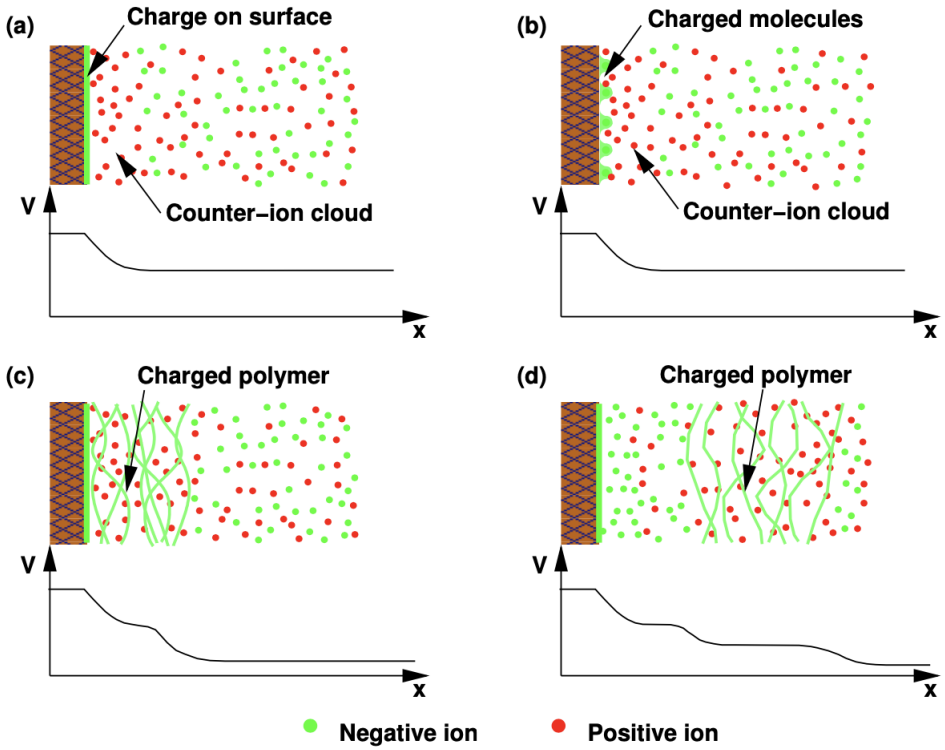

Figure 3.4: Charge distribution in the various electrodes for CapMix application: (a) electrode initially charged by an external power supply; (b) charged adsorbed molecules on the electrode surface; (c) surface coated with charged polymers; (d) electrodes coated by membranes. [3]

An electrical double layer forms in every scenario, but its structure is different. In case (a), charges are located inside the electrode; in case (b), they are on the surface; in case (c) they are distributed close to the electrode; in case (d) they are separated from the electrode.

Taking case (a) as an example, an analysis of charges distribution can be performed. The electrode potential $\Phi(\sigma, c_S)$ (w.r.t. the bulk solution) can be expressed as a function of the surface charge density σ and salt concentration inside the solution [3]:

$$\varphi_{GCS}(\sigma, c_S) = 2\frac{RT}{F} sinh^{-1}(\frac{\sigma}{\sqrt{8\epsilon_0\epsilon_r c_S RT}}) + \frac{\sigma}{C_{St}} \tag{3.5}$$

where ϵ_0 is the dielectric constant, ϵ_r is the relative permittivity of the solvent

and C_{st} is the specicfic Stern capacitance ($0.1\mathrm{F}/m^2$). This specific formula refers to flat electrodes and assumes point-like charges, but it can be further modified if porous materials are taken into account. If the pores are small, the potential is assumed uniform inside them, and its dependence on salt concentration can be expressed as [3]:

$$\varphi_{GCS}(\sigma, c_S) = \frac{RT}{F} sinh^{-1}(\frac{\rho}{2c_S F}) + \frac{\rho}{C_{St,Vol}} \tag{3.6}$$

where $C_{St,Vol}$ is the specific volumetric capacitance of the Stern layer (typical value $75 \cdot 10^6 F/m^3$) and ρ is the volumetric charge density. If the salt concentration or the charge in the EDL change, the potential of the electrode with respect to the solution changes; therefore, also a voltage rise appears. If we assume that the charge in the EDL is constant, then the voltage variation depends only on the salt concentration.

3.2.1 Activated Carbon

Activated carbon (AC) was the first carbon-based material used as a supercapacitor electrode. It is a form of disorder carbon with small pores and high surface area; in this way, a very high specific capacitance can be obtained, well suited for SC applications. AC sources can be found in wood, leaves, corn grain, coal, lignite and sugar cane, which makes this material very easy to obtain and low cost [15]. Usually a thermal or physical activation is performed to synthesize ACs materials [15] and consists in two steps:

- carbonization of the precursor: removal of non-carbon materials through thermal decomposition (700-1200°C) in oxidizing ambient (H_2O, CO_2 or air)

- gasification: partial etching of carbon during annealing process

Another type of activation is a chemical activation, which makes use of chemical reagents (KOH, H_2SO_4, etc...). In both cases, pores of different sizes can be obtained, ranging from macropores (> 50 nm), mesopores (2-50 nm) and micropores (< 2 nm) [15].

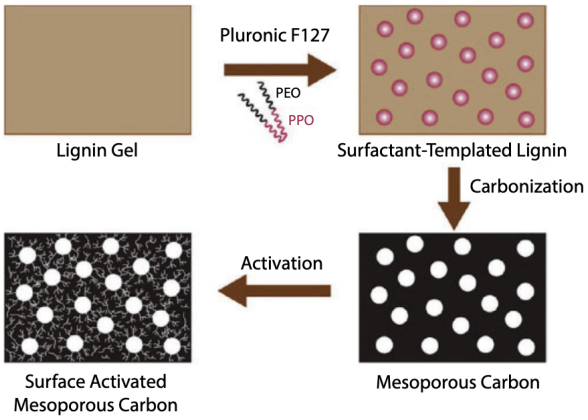

Figure 3.5: Example of a mesoporous AC extracted from a lignite precursor [15]

3.2.2 Carbon Nanotubes

Carbon nanotubes are graphene tubes with a diameter of a few Å and length of few μm [15]. There are three CNT structures available: single walled CNT (SW-CNT), double walled CNT (DW-CNT) and multi walled CNT (MW-CNT). SW-CNTs are obtained by rolling a single graphene sheet; they are highly flexible but not so easy to manage since they tend to from bundles [12]. DW-CNTs present an additional graphene rolled over the first tube. If a third or more sheets are rolled over the two core tubes, then MW-CNTs are created; they are much longer and occupy more volume than SW-CNTs, but they offer a higher resistance [12]. These three configurations are reported in figure 5.

Furthermore, CNTs can be distinguished by the hexagonal lattice orientation with respect to the axis. To do so, a chiral vector and chiral indices (n,m) are defined. Figure 5.a reports the three main structures: chiral (m≠n), armchiral (m=n), and zigzag (m=0). CNTs can be produced by chemical vapor deposition assisted by catalysts using methan, acetylane and propylene as precursors.

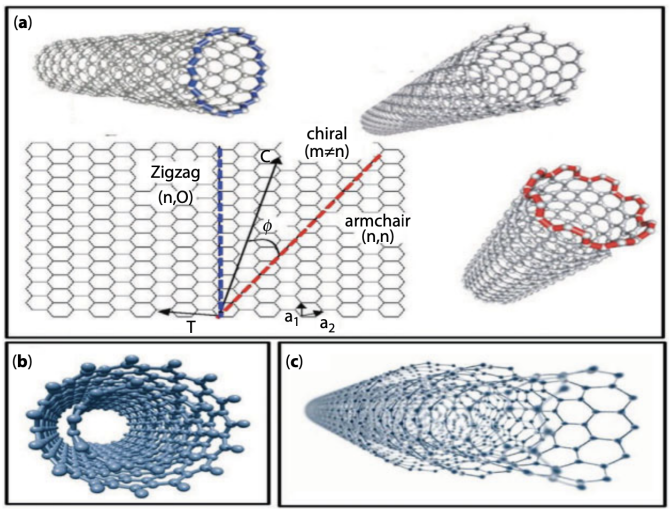

Figure 3.6: Examples of carbon nanotubes structures [15]. (a) SW-CNT (b) DW-CNT (c) MW-CNT

These nanostructures are characterized by a really high conductivity, good thermal and mechanical stability. They perform a great conductivity since there is no heating during conduction; this happens because conduction in CNTs happens due to ballistic transport, where charges do not collide with each other (no scattering) and have a relative high mean free path.
One of the drawbacks is that they have very low surface area with respect to other carobon-based electrodes (in particular activated carbon). To overcome this problem, CNTs can be functionalized by attaching some functional groups to the outer surface. The surface can undergo covalent or non-covalent modifications. A covalent modification consists in attaching polymer chains to the CNT by forming chemical bonds; this process modifies and ruins surface electronic properties. With non-covalent modifications, the polymer chains are attached to the CNT surface by adsorption of surfactant molecules; therefore, no chemical bond is formed in this case.

3.2.3 Carbon Nanofibre

Carbon Nanofibres (CNFs) are tower-like structure obtained by stacking graphene sheets one by one. They can be produced with electrospinning, chemical vapor deposition or pyrolysis of biomaterial [12]. CNFs electrochemical behaviour can be improved by adding a conducting or pseudocapacitive material, while the electrical conductivity can be enhanced by integrating metal nanoparticles or CNTs to the main structure [12].

3.2.4 Graphene

Graphene is a one atom thick layer of carbon atoms. It is characterized by a high specific surface area ($\approx$ 2630 m^2/g) and a high intrinsic specific capacitance ($\approx$ 550 F/g), making it very suitable for SC applications [15]. Advantages include high flexibility, low ion transport diffusion resistance, while a big disadvantage consists in its tendency to agglomerate, causing a limitation of ion diffusion that limits the electrochemical performance. In particular, this phenomenon drastically reduces the specific surface area where the EDL can form, therefore reducing the actual amount of charge that can be stored. This main problem can be solved by introducing a spacer between the electrodes, avoiding the stacking of the two materials.

3.2.5 Fullerene

Fullerenes are structural spheres made of pentagonal and hexagonal rings of carbon atoms. They are characterized by high conductivity and a small bandgap, which allow a really high charge transfer. Fullerenes can be combined with other types of materials such as metal oxides and conductive polymers to modify ion diffusion and electron transport properties.

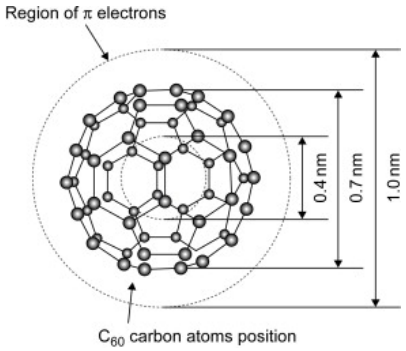

Figure 3.7: An example of fullerene structure [16]

3.3 Electrolytes

The electrolyte is formed by the electrolyte salt and the solvent. It is fundamental for the EDL process since it supplies ionic conductivity making easier the EDL formation process. Furthermore, the electrolyte choice strongly influences performance parameters (capacitance and pseudocapacitance, operational voltage, power and energy density). The variables that must be monitroed are:

- ion type and size

- ion concentration
- solvent
- interaction between the ion and the solvent
- interaction between the electrolyte and the electrode materials

Figure 3.8 shows a classification of the main types of electrolytes. In particular, the principal division is between liquid and solid electrolytes; then, liquid electrolytes are divided in aqueous electrolytes, organic electrolytes and ionic liquids.

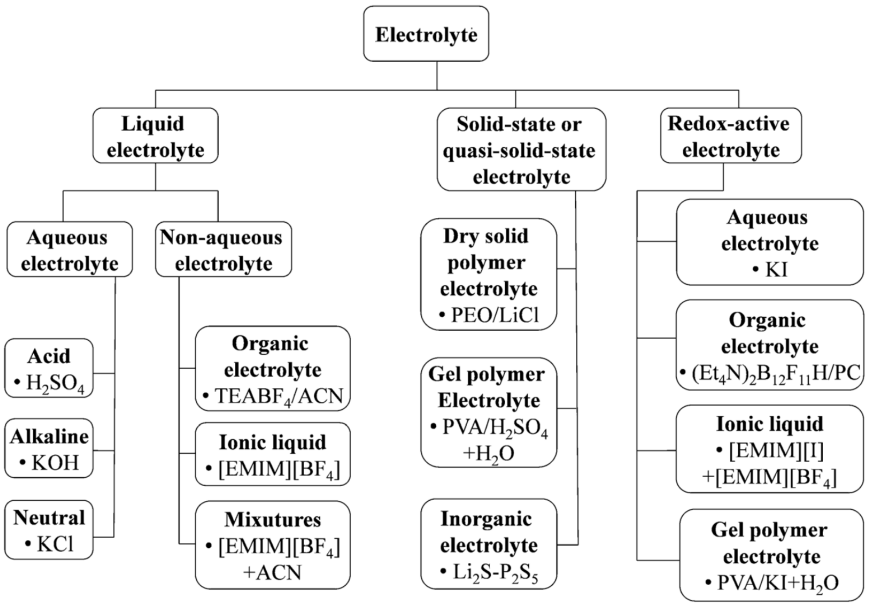

Figure 3.8: Classification of electrolytes for SCs [17]

3.3.1 Aqueous electrolytes

Aqueous electrolytes are cheap and easy to manage, meaning that laboratory experiments and fabrication processes are facilitated, and exhibit a higher conductivity than organic and ionic liquid electrolytes . However, these types of electrolytes present a narrower voltage range than the others, meaning that most commercial devices don't use them very often. Aqueous electrolytes can be grouped into three subcategories:

- acid: H_2SO_4 is the most used acid electrolyte; it is characterized by a high ionic conductivity which of course depends on concentration (0.8 S/cm for 1 M H_2SO_4 at 25°C [17]). ESR is lower than neutral and alkaline electrolytes, while specific capacitance is higher.

- alkaline: KOH is the most popular choice due to its high conductivity (0.6 S/cm for 6 M at 25°C [17]); also other alkaline materials like NaOH and LiOH are used.
- neutral solution: the most used neutral electrolytes are based on Mg, K and Li salts; they are characterized by greater safety, less corrosion and larger operating voltage. Since they have lower ionic conductivities, they exhibit lower specific capacitance and higher ESR; anyway, they can perform in a larger potential window and can be managed with much more safety than acid or alkaline electrolytes [17].

3.4 Separators

The separator is needed in a SC cell in order to separate physically the electrodes and prevent that electrons transfer between anode and cathode. These device parts must be chosen taking into account these three requirements:

1. they must have a low resistance for ion transfer but they must be a good electronic insulator
2. they must be chemically and electrochemically stable in the electrolyte
3. they must exhibit a good durability

Separators materials include porous films and membranes like cellulose, glass fibres and polymer membranes; the choice among them depends on the cell voltage, cell temperature and type of the electrode. Moreover, separators must be chosen carefully since their properties (material composition, porosity, thickness) influence performance parameters of a SC cell like specific capacitance, ESR, specific power and energy densities [17].

Chapter 4

Methods

This chapter describes the most used methods to evaluate the performance of a supercapacitor. In particular, three key parameters have to be monitored are the cell total capacitance C_T, the operating voltage V_o and the equivalent series resistance R_{ES} [11]. Those values are useful to determine the energy and power production capability and are usually exploited to fully characterize commercial products since the design, fabrication and material choice is fixed.
Figure 4.1 shows a diagram where all parameters, principal affecting factors and calculation methods are presented.

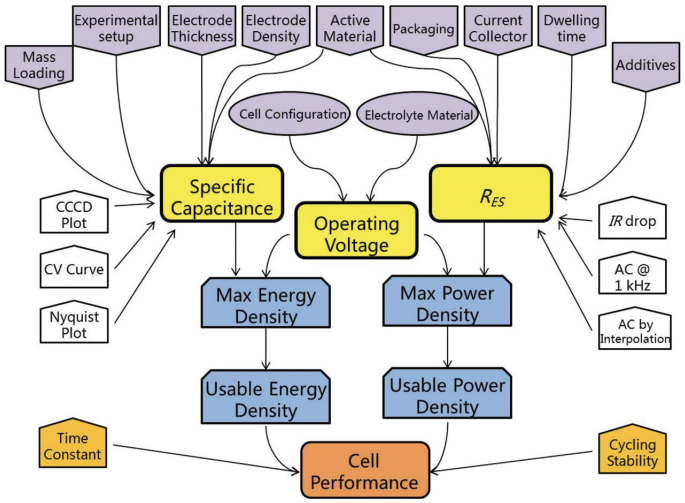

Figure 4.1: Schematics of key test methods, performance metrics and major affecting factors for the evaluation of supercapacitors performance [11]

The yellow regions are the three key parameters, the blue ones are related to power and energy density, cycling stability and time constant are in light orange.

All the main affecting factors are indicated with a purple color.
Finally, white boxes illustrate all the principal measurement techniques that are needed to test the cell performance. In particular, cyclic voltammetry (CV), constant current charge/discharge (CCCD) and electrochemical impedance spectroscopy (EIS) tests are the most used in this experimental field. These methods are employed to find voltage, current, and time, which are the basic quantities; more complex quantities, like capacitance, series resistance, operating voltage, time constant, power and energy are derived from the first three basic values.

4.1 Configurations

There are two main configurations that are employed to conduct measurements on SC devices: three-electrode configuration and two-electrode configuration. The choice between them depends on the type of electrode, electrolyte, separator and current collector employed.

The three-electrode configuration makes use of a working electrode (the material that has to be studied), a reference electrode (usually Ag/AgCl) and a counter electrode (Platinum). The measurement process is done by inserting these three electrodes inside the chosen electrolyte; usually it is used to characterize the electrochemical behaviour of a material, including finding the presence/absence of redox reactions and studying kinetic/diffusion process at the electrode surface. Three-electrode structure is not suitable for capacitance, energy and power density calculation [18].

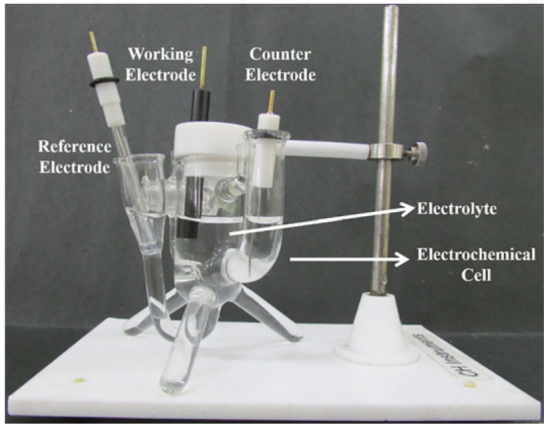

Figure 4.2: Three-electrode configuration [18]

The two-electrode configuration makes use of only two electrodes, constituted

by two active materials coated on the current collectors. A separator is soaked with the electrolyte solution and then sandwiched between the electrodes. This structure is generally used to obtain a reliable value of capacitance, energy and power densities since it is similar to a supercapacitor prototype structure [18].

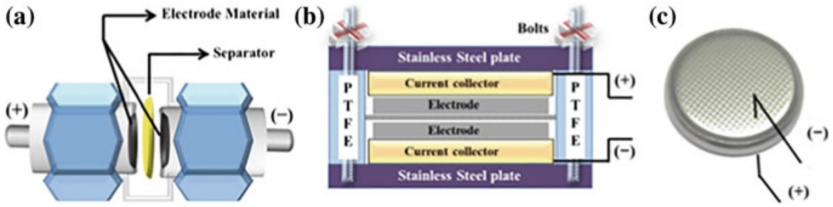

Figure 4.3: Schematics of several two-electrode configurations [18]

4.2 CV: Cyclic Voltammetry

Cyclic Voltammetry cyclically applies a voltage to a cell and consequently measures the current that flows in the cell. If this technique is used on a two-electrode system, then the voltage is applied between the positive and negative electrodes; if a three-electrode is tested, then the voltage is applied between the working electrode and the reference electrode. The speed of this potential change is called "sweep rate" or "scan rate" (ν) and it is referred in mV/s; the potential range, instead, is called "operating window" or "potential window". The current collected from a CV is able to describe if and how chemical reactions occur in the SC [11]. Usually a CV is displayed in a current (A) VS potential (V) or current (A)/potential (V) VS time (s) graph; the latter is reported on figure 4.4.

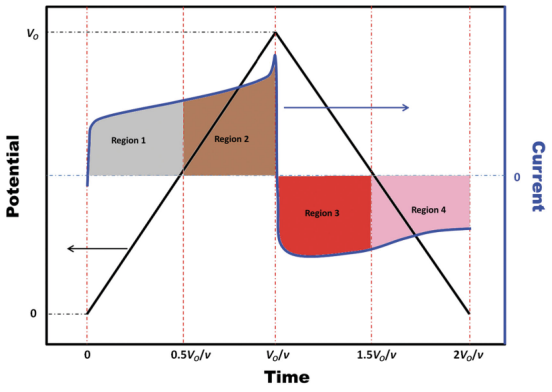

Figure 4.4: Typical CV test result [11]

Obviously, different materials produce different CV results depending on the mechanism that allows to store the charge.

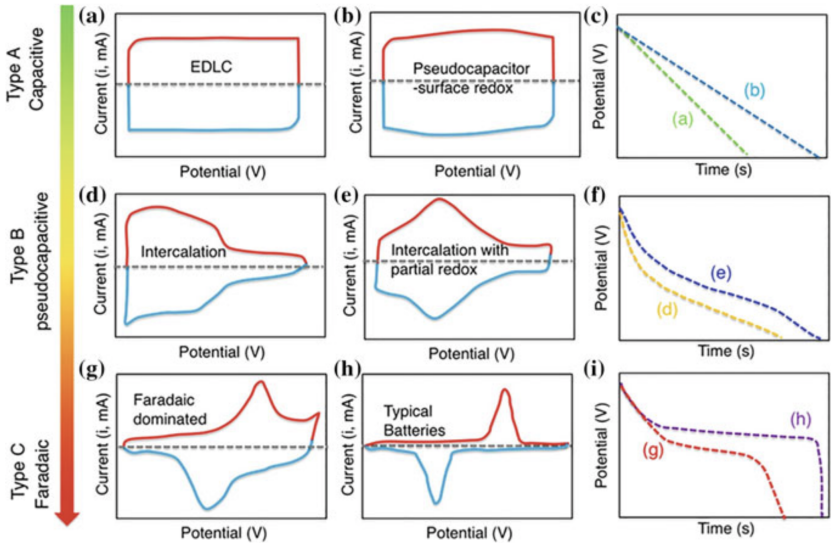

Figure 4.5: (a, b, d, e, g, h) Schematic cyclic voltammograms and (c, f, i) corresponding galvanostatic discharge curves for different energy storage materials. [18]

Figure 4.5 shows CVs and constant current charge–discharge for different types of materials (capacitive, pseudocapacitive and faradic). EDL capacitors, which are the ones we are interested in, exhibit an almost perfectly rectangular shape; pseudocapacitors have pronounced redox peaks in their CV [11]. However, some pseudocapacitive materials have a very similar shape to the EDL ones, so it is usually difficult to define the type of material only by looking the voltammetry graph. Figures 4.5 (c, f, i) can be helpful, since a linear current response can be found only in EDL capacitors [18]. In fact, the instantaneous current induced by the EDL mechanism is proportional to the scan rate, while the one generated by the PC mechanism is proportional to the square root of the scan rate [11].
Finally, cyclic voltammetry can be helpful to evaluate the operating voltage or potential window for SCs by repeatedly adjusting the reversal potential in the measuring system. The CV curves can be integrated to find capacitance and energy related parameters [11].

4.3 EIS: Electrochemical Impedance Spectroscopy

Electrochemical Impedance Spectroscopy applies an alternating voltage with small amplitude (normally 5mV [11]) superimposed to a steady-state potential to study the frequency response of a system (typically between 0.01 and 1000Hz [18]). The results of these measurements are displayed in a Bode plot or in a Nyquist plot; the former shows the relation between the phase angle and the frequency, while the latter displays in a complex plane the real and imaginary parts of the impedance of the device. This method can be used to measure the effective series resistance of a supercapacitor, charge transfer, mass transport or specific capacitance [11].

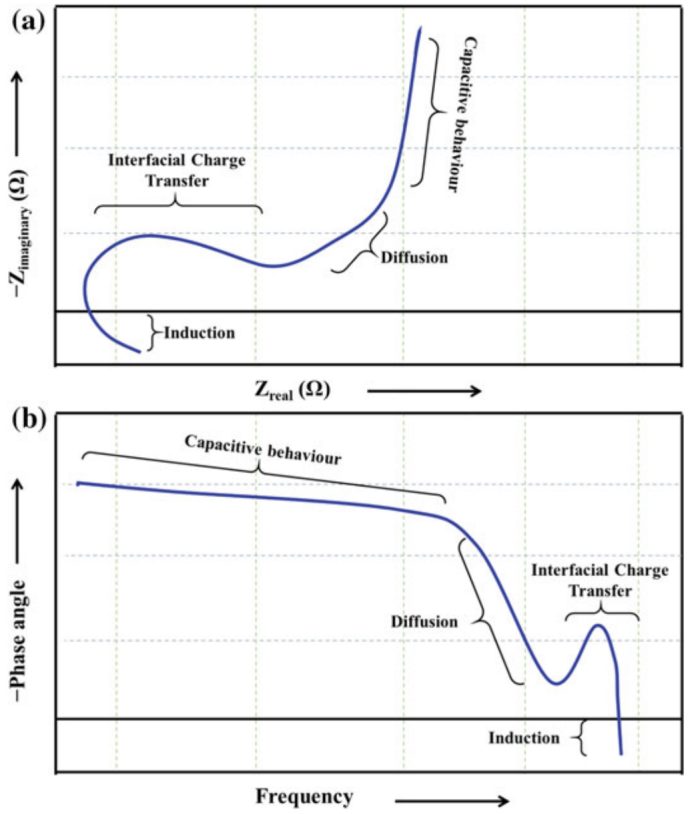

Figure 4.6: (a) Nyquist and (b) Bode plots examples for supercapacitors [18]

Figure 4.6 shows an example of Bode and Nyquist plots derived from EIS measurements. In particular, the Nyquist plot has three distinguished zones of the spectra: a semicircular zone for high frequencies, a linear part with 45° slope (called the Warburg element at mid-frequency/knee frequency zone [18]) and another linear portion with very high slope corresponding to the double-layer capacitance.

Sometimes, there could be a fourth portion called inductive tail, due to inductive effects between the electrodes related to anomalous magnetism present on edge atoms [18]. For ideal double-layer capacitors, which should have a total capacitive behaviour, only a straight line should appear in the Nyquist plot; this line coincides with the positive imaginary impedance axis and intercepts the real impedance axis at the origin (no resistance) [18]. The Bode plot, instead, should have a gradual increase of the phase angle until it stabilizes to a value of 90°.

4.4 CCCD: Constant Current Charge/Discharge

Constant Current Charge/Discharge is a technique that consists in repeatedly charging and discharging a SC at a specific current level. The results are displayed in a potential (V) VS time (s) graph, like in figures 4.7a and 4.7b.

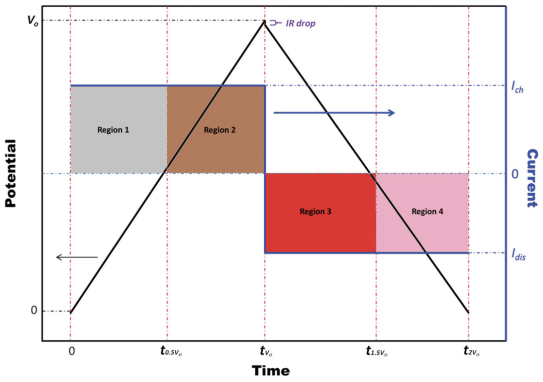

(a) Linear potential change over time

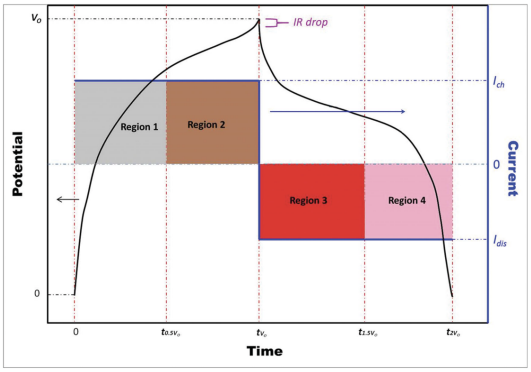

(b) Nonlinear potential change over time

Figure 4.7: CCCD test results of a SC [11]

CCCD is the most used technique to characterize a supercapacitor, since all

three key parameters can be obtained from this measurement (C_T, R_{es}, V_o) [11]. Also, all the other properties can be calculated from these quantities, such as energy and power densities, time constant, leakage current.

4.5 Key Parameters

4.5.1 Capacitance

The evaluation of the device capacitance can be performed with both two-electrode and three-electrode systems. Usually, the former is used with a complete supercapacitor device, while the latter is preferred to study single electrodes and materials [18].
The total capacitance C_T of a SC is

$$C_T = \frac{\Delta Q}{\Delta V} \tag{4.1}$$

where ΔV is the applied potential and ΔQ is the charge. If the specific capacitance is needed, the C_T is then divided by a Π parameter:

$$C_S = \frac{\Delta Q}{\Pi \Delta V} \tag{4.2}$$

where Π could refer to volume, mass, area, or length [18]. The specific capacitance would be then called respectively volumetric (F/mL), gravimetric (F/g), areal (F/cm^2) or linear (F/cm). If C_S is normalized by the cell volume or weight, it can be used to describe the device performance [11].

Capacitance Evaluation

The total cell capacitance can be derived by integrating under the CV curve with the following formula:

$$C_T = \frac{\Delta Q}{\Delta V} = \frac{\int_0^{\frac{2V_o}{\nu}} i(V)dV}{2V_o} \tag{4.3}$$

where ν is the potential sweep rate [11].
CCCD allows an easier extrapolation of the capacitance from its data. The expression used is the following:

$$C_T = \frac{I}{\frac{\Delta V}{\Delta t}} = \frac{I\Delta t}{\Delta V} \tag{4.4}$$

where I is the constant current applied, while $\Delta V/\Delta t$ is the slope of the potential discharge curve [18]. Finally, capacitance can be calculated also from EIS:

$$C_{Tf} = \frac{1}{2\pi f x Im(Z)} \tag{4.5}$$

where C_{Tf} is the capacitance value at frequency f of the superimposed AC signal and Z is the complex impedance value [18]. Equation 4.5 is effective when low frequency signals are applied during EIS test. From [11], another way to calculate the capacitance is with the following equations:

$$Re(C) = \frac{-Im(Z)}{\omega|Z|^2} \tag{4.6}$$

$$Im(C) = \frac{Re(Z)}{\omega|Z|^2} \tag{4.7}$$

where $Z = Re(Z)^2 + Im(Z)^2$ is the complex impedance, $\omega = 2\pi f$ is the angular velocity, and Re(C) and Im(C) are respectively the real and imaginary capacitances [11]. Re(C) indicates the energy stored, thus can be used to describe the capacitance C_T of the cell, while Im(C) describes the energy dissipation of the device.

Specific Capacitance Evaluation

After calculating C_T, then C_S can be obtained using equation 4.2. From [11], it is known that the specific capacitance value obtained depends on the type of measuring system that is considered. In particular, figure 4.8 shows three common setups: symmetric two-electrode (b), asymmetric two-electrode (c) and three electrode (a) configurations.

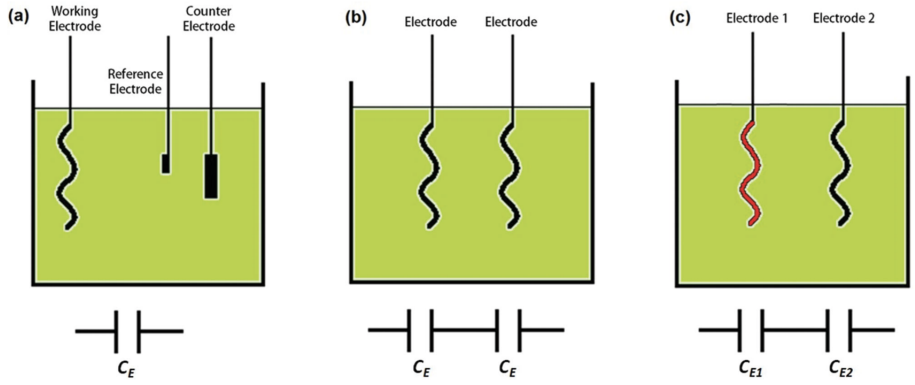

Figure 4.8: Sketches and equivalent circuits of three different experimental setups [11]

A brief example with gravimetric C_S is illustrated to show this peculiarity. The weight of each electrode is m, while for the asymmetric electrodes they are m_1 and m_2; also, the electrode capacitance is C_E. From [11], gravimetric C_S for each case is:

$$C_{Sa} = \frac{C_E}{m} \tag{4.8}$$

$$C_{Sb} = \frac{1}{4}\frac{C_E}{m} \tag{4.9}$$

$$C_{Sc} = \frac{1}{2(1+\alpha)}\frac{C_E}{m} \tag{4.10}$$

where $0 < \alpha < 1$ is a fraction of electrode 2 mass.

4.5.2 Equivalent Series Resistance

A real SC device has an internal resistance, so a part of the energy that is stored inside it is dissipated. SC can be depicted as a system of a capacitance C_T and a resistance R_{es} in series (figure 4.9).

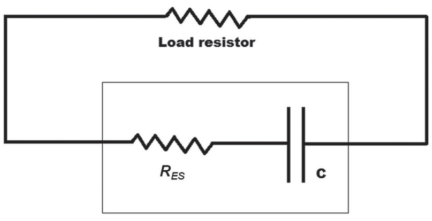

Figure 4.9: Equivalent series RC circuit for a SC [11]

The equivalent series resistance (RES)can be derived from CCCD test by applying the Ohm's law to the IR drop:

$$R_{es} = \frac{\Delta V}{\Delta I} \tag{4.11}$$

where ΔV and ΔI are the voltage and current of the IR drop. EIS can be also useful to find R_{es}. It is the real part of the complex impedance evaluated at 1kHz, or it can be extrapolated by interpolation of the low frequency part of the Nyquist plot (Im(Z) = 0) [11]. Both methods are described in figure 4.10.

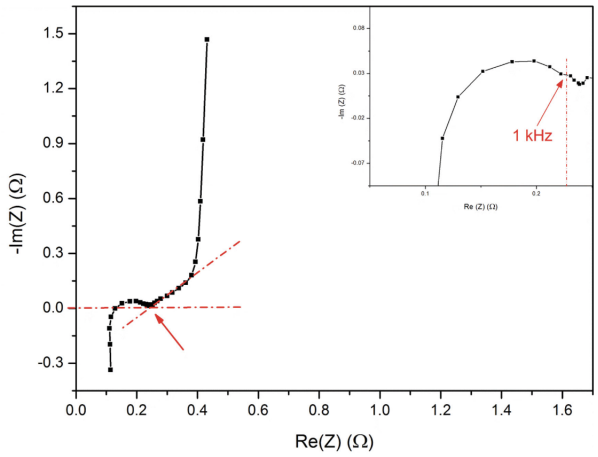

Figure 4.10: RES determination methods [11]

4.5.3 Operating Voltage

The operating voltage V_o is the voltage range within the cell is able to work properly. It is associated to a potential window, which is the potential range where an electrode normally operates. If voltage values are higher than the operating voltage, the cell or the electrodes (or both) could be irreversibly destroyed.

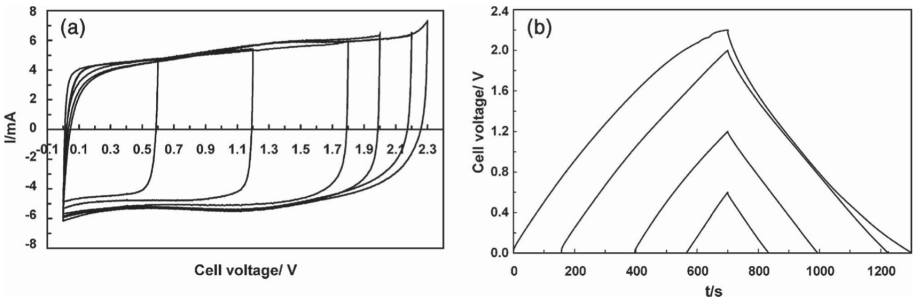

Figure 4.11: V_o determination methods [11]

In figure 4.11, it can be seen that both CV and CCCD can be used to define the operating voltage. Usually the measurement starts with a lower voltage value, and then it slowly increases until a spike appears at the boundary of the potential window [11]. The operating voltage is limited by the cell configuration and by the solvent in electrolytes. In an aqueous solution, voltage can be up to 1 V due to thermodynamic decomposition potential of water at room temperature [11]. For what concerns the cell design, an asymmetric system can be exploited: using

different materials for the electrodes causes an additional electrochemical potential difference, and V_o can reach up to 2-2.3 V [11].

4.5.4 Time Constant

A supercapacitor has an internal resistance modeled by R_{es} like in figure 4.9. Therefore, since both a resistance and a capacitance are present in a real SC device, also a time constant can be defined:

$$\tau = R_{es} C_T \tag{4.12}$$

The smaller the τ, the better the device performance. Generally, for most commercial SCs, τ ranges from 0.5 to 3.6 seconds [11].

4.5.5 Energy density

The energy density is the electrical energy that a device is able to store or release. Stored energy is obtained by integrating the charging curve, while released energy is calculated by integrating the discharging curve. These values can be normalized in terms of mass loaded on the electrode (gravimetric energy - Wh/Kg) or volume of the electrode (volumetric energy - Wh/L) [18]. The specific energy can be calculated from CV data as:

$$E_S = \frac{1}{2} C_S \Delta V^2 \tag{4.13}$$

where C_S is the specific capacitance and ΔV is the potential difference [18]. Another simple way to evaluate the energy of an EDLC device is from the CCCD test, since for such systems the charge/discharge curve is linear, so an integration is sufficient:

$$E_S = \int_0^Q V_o dq = \frac{1}{2} V_o Q = \frac{1}{2} V_o I t_c \tag{4.14}$$

where Q is the charge in the system after an application of a constant current I over a time t_c [18]. The result is expressed in Joules: to have watt-hour values, a simple division by a factor 3600 can be done.

4.5.6 Power density

Power density defines how quickly the energy of a device is consumed/produced. It is generally measured gravimetrically (W/Kg) or volumetrically (W/L) and can be derived from capacitance values [18].

The following equation calculates specific power using R_{es} (obtained both from IR drop in CCCD or EIS):

$$P_S = \frac{V_o^2}{R_{es}\Pi} \tag{4.15}$$

where V_o is the operating voltage [11]. If CV data are available, power can be obtained as:

$$P_S = \frac{1}{2}C_S\Delta V\nu = \frac{1}{2}V_oI \tag{4.16}$$

Finally, for symmetric CCCD curves, power can be obtained from energy density:

$$P_S = \frac{E_S^{CCCD}}{\tau_d} \tag{4.17}$$

where τ_d is the charging/discharging time constant of the device.

4.5.7 Coulombic Efficiency

The Coulombic efficiency is a parameter that describes how much charge is lost during a charge/discharge cycle. It is defined as the ratio between the charge released during the discharging phase over the charge stored during the charging phase:

$$\eta = \frac{Q_{discharge}}{Q_{charge}} \tag{4.18}$$

The ideal value is 1, but generally SCs have an efficiency lower than 1 due to power dissipation of the internal resistance of the device [19].

Chapter 5

CNT electrodes: electrochemical characterization

In this chapter, electrochemical measurements are performed on carbon nanotube samples to obtain data on the efficiency of the material in salt solutions. Some of these samples are modified with electrochemical functionalizations to improve their performance for higher potential values.

A DexMat CNT film is used (1 cm wide and 1 m long) as a test material and it is cut in 1cm x 1cm pieces to conduct separate analysis.
A three-electrode configuration is chosen, where the reference electrode is an Ag/AgCl electrode, the counter electrode is made of a titanium stripe with activated carbon on the edge, and the working electrode is the CNT tape attached to a titanium stripe. The electrolyte is a NaCl solution with 1M concentration.

5.1 Not activated CNT tape

The first measurements are taken on not activated samples. The tape is put in the solution for about an hour in order to let the OCP stabilize. In this case, the OCP is around 100 mV. Then, several CVs are performed for different values of applied potential VS OCP. Figure 5.1 shows the resulting curves in the potential window [-500 mV, 500 mV] VS ref, since SC devices in CapMix applications normally operate within this range.

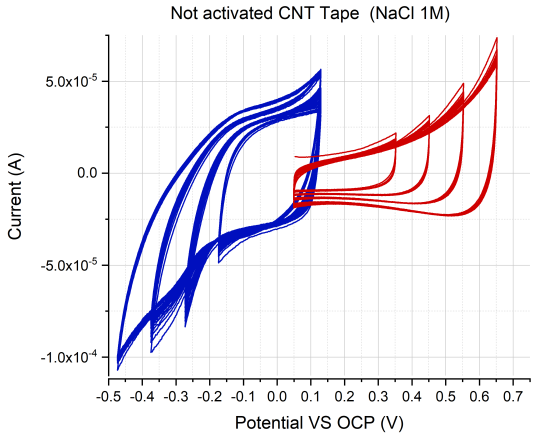

Figure 5.1: CVs of not activated CNT tape (NaCl 1M solution; 1cm x 1cm area)

It can be seen that the CV shapes for the anodic window are quite good, with an almost rectangular form meaning that the electrode has a good capacitive behaviour. However, the cathodic CVs exhibit some current spikes which become higher and higher when a larger potential value is applied, meaning that the cell would not work properly at those polarizations.
The coulombic efficiency for each potential applied is caluclated; the results (figure 5.2) confirm the considerations done on the CV graph.

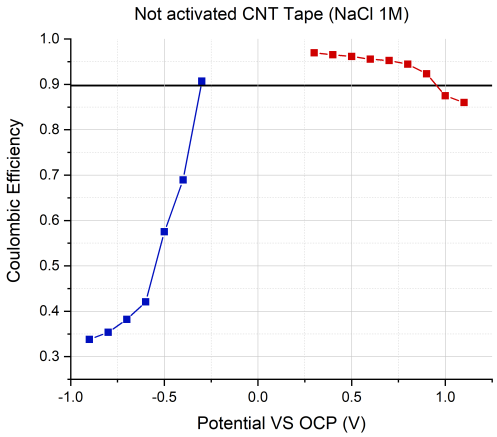

Figure 5.2: Coulombic efficiency of not activated CNT tape (NaCl 1M solution; 1cm x 1cm area)

The tape performs very efficiently in anodic polarizations ($\eta > 90$ %), while the efficiency for negative values of potential drastically drops to very low levels. The

potential window for this material with NaCl 1M solution as an electrolyte is [-0.3 V, 0.9 V] VS OCP.

5.2 CNT tape: functionalizations

To improve the performance of the CNT electrode (for the cathodic window in particular), some activation processes are performed to the tape. Three different functionalizations are chosen:

A. The tape is immersed in KOH for 2 hours and then it is put 30 minutes in a sonicator. After that, an electrochemical activation (several CVs) is performed in HNO_3 1M.

B. The tape is immersed for 2 hours in a solution of sulfuric acid (H_2SO_4) and nitric acid (HNO_3) with ratio 2:1.

C. The tape is immersed for 2 hours in a solution of ethanol (C_2H_6O) and nitric acid (HNO_3), where the former is 3% in volume with respect to the latter.

5.2.1 First functionalization (KOH + HNO_3)

The first activation is performed with KOH and HNO_3. Figure 5.3 shows that the sample has a good capacitive behaviour both for anodic and cathodic windows.

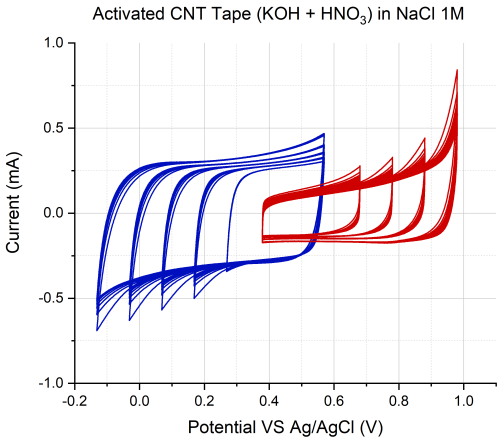

Figure 5.3: CVs of CNT tape activated with KOH and HNO_3 (NaCl 1M solution; 1cm x 1cm area)

The efficiency calculated and reported in figure 5.4 clearly shows that the tape now works better also in cathodic window, while the efficiency values for the anodic window still remain high.

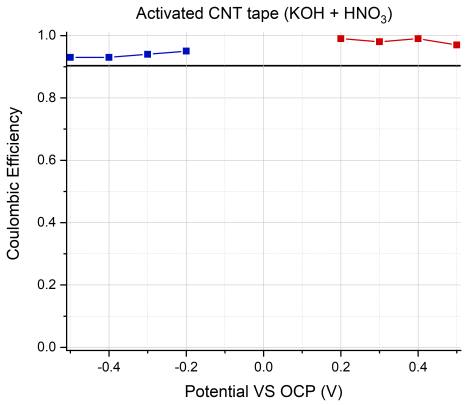

Figure 5.4: Coulombic efficiency of CNT tape activated with KOH and HNO_3 (NaCl 1M solution; 1cm x 1cm area)

5.2.2 Second functionalization (HNO_3 + H_2SO_4)

The second functionalization makes use of a solution of HNO_3 and H_2SO_4. After 2 hours in sulfuric and nitric acid, the tape surface looks degraded due to the aggressive action of the two compounds. Anyway, it is still tested with some measurements and the results are in figure 5.5.

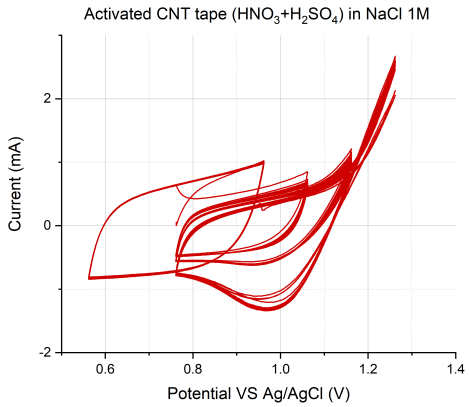

Figure 5.5: CVs of CNT tape activated with H_2SO_4 and HNO_3 (NaCl 1M solution; 1cm x 1cm area)

The sample shows a more ohmic behaviour with respect to the other cases. Also, there are some spikes on the upper right part of the plot. The tape doesn't have a good capacitive behaviour, and this is confirmed also by figure 5.6, where the efficiency already drops below 90% after 400 mV VS OCP.

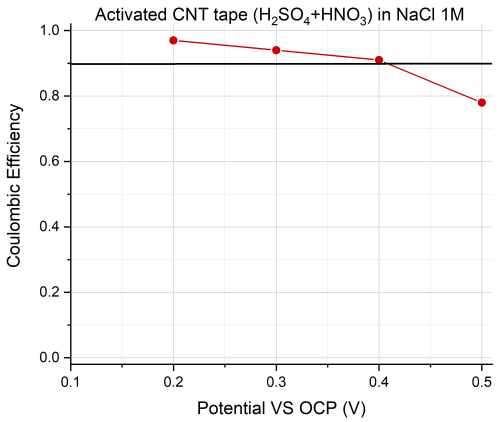

Figure 5.6: Coulombic efficiency of CNT tape activated with H_2SO_4 and HNO_3 (NaCl 1M solution; 1cm x 1cm area)

5.2.3 Third functionalization (HNO_3 + C_2H_6O)

For the last functionalization, a solution of HNO_3 and C_2H_6O is used. The tape is immersed in this solution for 2 hours, and then some CVs are taken. An anodic analysis is performed to verify if an efficiency higher than the not activated tape can be found.
After 2 hours in the solution, the tape results less degraded than the tape activated with sulfuric and nitric acid. The CV graph in figure 5.7 reveals that this activated sample exhibits a good capacitive behaviour, with the CV having rectangular shapes.

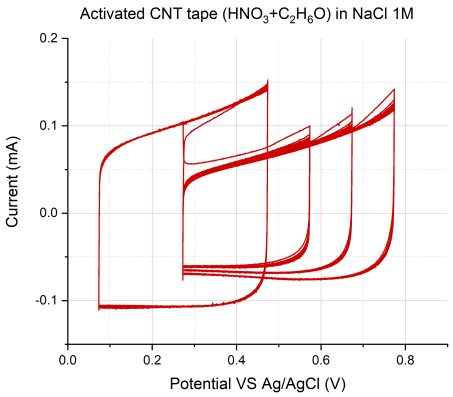

Figure 5.7: CVs of CNT tape activated with C_2H_6O and HNO_3 (NaCl 1M solution; 1cm x 1cm area)

The coulombic efficiencies reported in figure 5.8 are higher than the efficiencies reported for the not activated tape. In fact, for smaller voltages, $\eta \approx 99\%$.

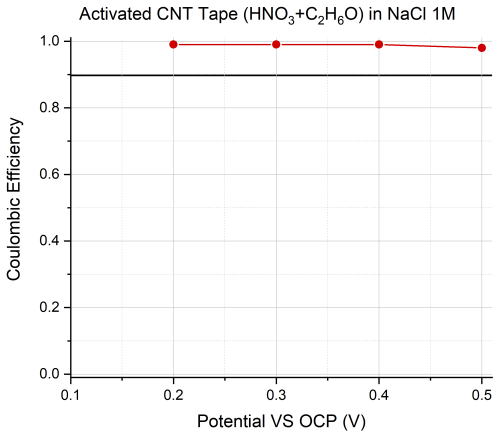

Figure 5.8: Coulombic efficiency of CNT tape activated with C_2H_6O and HNO_3 (NaCl 1M solution; 1cm x 1cm area)

5.2.4 Comparison

Figure 5.9 reports a comparison of the efficiencies of all the tapes studied. For the cathodic window, the KOH + HNO_3 activation performs much better than the not activated one, with values higher tham 90% up to -500 mV.

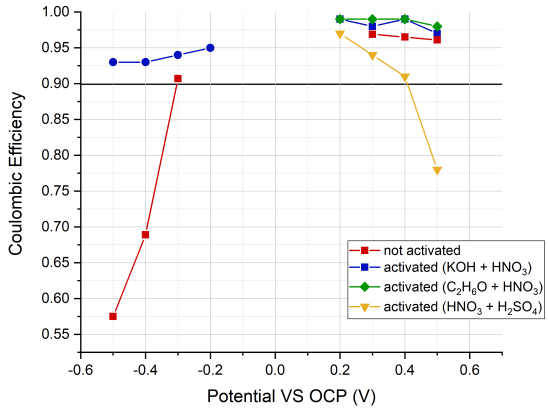

Figure 5.9: Coulombic efficiency comparison

The anodic window is also reported in a zoom in in figure 5.10. The HNO_3 + H_2SO_4 activation has the worst behaviour, while the other two activations perform better than the not activated sample, achieving efficiency values up to 99%.

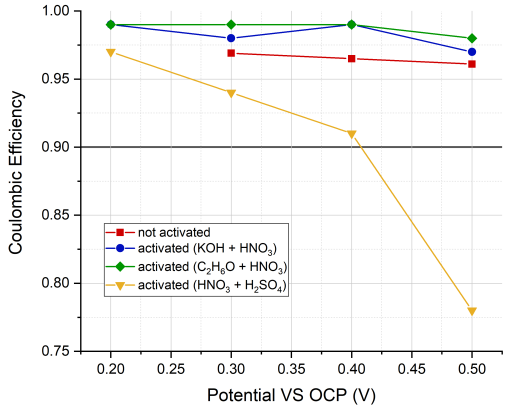

Figure 5.10: Coulombic efficiency comparison - zoom in

5.3 Potential rise

After calculating the potential windows and efficiencies, the potential rise is studied. As we know from chapter 2.2, when the CNT tape is immersed in a high salinity solution a low salinity solution is injected in the cell, a potential rise occurs.
In this section the potential rise of each functionalization is measured. For each kind of sample used, various potential values are applied VS the reference electrode, and for each potential applied the potential rise is measured.

5.3.1 NaCl solution

First of all, the measurements are taken in salt and fresh water. Two solutions are used to simulate these two types of water. For salt water, a solution of NaCl with 0.6 M concentration is chosen. For fresh water, a solution of NaCl with 10 mM concentration is utilized.
Three types of samples are chosen:

1. Not activated CNT tape: positive potentials are applied since from 5.2 only the anodic window presents good efficiency values.

2. Activated CNT tape ($C_2H_6O_2$ + HNO_3): both positive and negative potentials are examined; from 5.8, the anodic window has an excellent efficiency, therefore a good behaviour in anodic conditions is hopefully expected.

3. Activated CNT tape (KOH + HNO_3): negative potentials are examined; from 5.4, a good cathodic behaviour is expected also in this measurement.

The HNO_3 + H_2SO_4 activation is not considered anymore due to its poor capacitive behaviour. In all three cases, the electrode is immersed in the high salinity solution for about an hour to let the OCP stabilize. After that, a potential is applied for 15 minutes and then salt water is replaced by fresh water. A potential rise is observed while the electrode stays in the low salinity solution. The electrode is put again in salt water and the potential is reapplied for 5 minutes to check if then the potential rise value changes or stays the same as the previous cycle. For every potential applied, four measurements cycles are performed. The potential step is 100 mV.
The results are in figures 5.11 and 5.12.

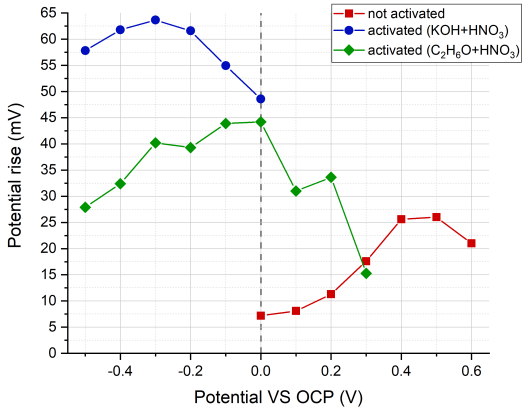

Figure 5.11: Potential rise of CNT tapes for different values of potential vs OCP

Figure 5.11 shows the potential rises of the three electrodes that are function of the potential applied vs OCP. From this graph it is already clear that the activated tape with KOH and HNO_3 has the best results in terms of potential rise value. Meanwhile, the not activated tape has the worst values. A more precise comparison can be done by looking at figure 5.12, where the same potential rises are displayed but in this case the x axis shows the potential applied vs the Ag/AgCl reference electrode.

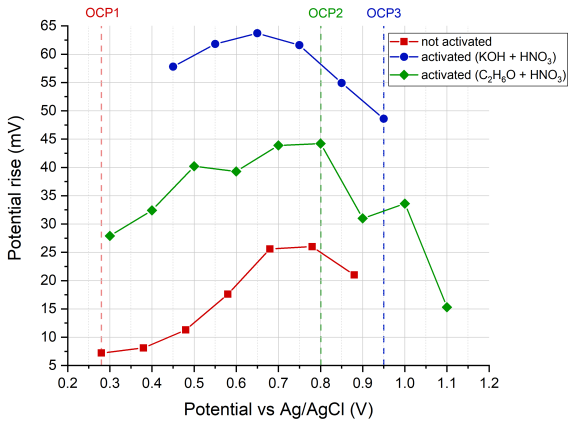

Figure 5.12: Potential rise of CNT tapes for different values of potential vs Ag/AgCl reference electrode

The not activated tape has OCP1 = 280 mV; the one activated with KOH + HNO_3 has OCP2 = 800 mV; the last one, which is activated with C_2H_6O + HNO_3

has OCP3 = 950 mV.

5.3.2 Brine

The same procedure is now performed with a different electrolyte. After salt water and fresh water, brine is considered. Brine is a high-concentration solution of salts in water. The salinity of brines ranges from 3.5% (typical of seawater) to 26% (saturated brine) [20]. Evaporation of brines happens naturally but it is also exploited to mine different types of salt, including NaCl.

For diluted brine, 1M concentration is chosen. For 1L of solution, the compounds quantity is calculated and it is reported in table 5.1. An additional column reports the maximum molarity of the elements, meaning that a higher molarity would cause their precipitation. All the compounds are chosen with lower molarity, so precipitation doesn't occur. This procedure is done also for all the salt combinations that could form in the solutions (not reported).

Compound	**Quantity**	**Molarity**	**Maximum Molarity**
LiCl	1.05 mg	0.02 mM	19.6 M
NaF	2.2 mg	0.05 mM	1 M
$NaNO_3$	5.23 mg	0.06 mM	10.3 M
H_3BO_3	25.68 mg	0.4 mM	0.4 M
$SrBr_2$	27.05 mg	0.1 mM	0.75 M
NaBr	70.68 mg	0.68 mM	8.8 M
$NaHCO_3$	199.77 mg	2.37 mM	1.1 M
$CaCl_2$	252.3 mg	2.27 mM	6.7 M
K_2SO_4	870.45 mg	4.9 mM	0.6 M
Na_2SO_4	3.25 g	22.9 mM	3.1 M
$MgCl_2$	5.04 g	52.9 mM	5.7 M
NaCl	24.64 g	0.4M	6.1 M

Table 5.1: Brine compounds (1L 1M solution)

Table 5.2 shows the compounds quantities of the concentrated brine (1L 5M solution) which are five times the quantities of the diluted one. Also here the molarity is controlled to check the solubility.

Compound	Quantity	Molarity	Maximum Molarity
LiCl	5.25 mg	0.1 mM	19.6 M
NaF	11 mg	0.25 mM	1 M
$NaNO_3$	26.15 mg	0.3 mM	10.3 M
H_3BO_3	128.4 mg	2 mM	0.4 M
$SrBr_2$	135.25 mg	0.5 mM	0.75 M
NaBr	353.4 mg	3.4 mM	8.8 M
$NaHCO_3$	998.85 mg	11.9 mM	1.1 M
$CaCl_2$	1.26 g	11.4 mM	6.7 M
K_2SO_4	4.35 g	24.9 mM	0.6 M
Na_2SO_4	16.25 g	114.4 mM	3.1 M
$MgCl_2$	25.2 g	264.7 mM	5.7 M
NaCl	123.2 g	2.1 M	6.1 M

Table 5.2: Brine compounds (1L 5M solution)

The potential rise is measured as in the NaCl case. The CNT tape is put in the concentrated brine for 1 hour to let the OCP stabilize. After that, the diluted brine replaces the concentrated one and the potential rise is obtained. The same procedure is done for different potentials applied, and for each potential 4 cycles are performed. The three samples that are studied are:

1. Not activated CNT tape: an anodic analysis is performed since its cathodic window presents a low efficiency.

2. Activated CNT tape ($C_2H_6O_2$ + HNO_3): both positive and negative potential values are applied.

3. Activated CNT tape (KOH + HNO_3): cathodic analysis is performed.

The potential applied to the tapes has step 100 mV and it is applied in high salinity solution for 15 minutes. After the first cycle, the same potential is applied again but for 5 minutes. The result is shown in figure 5.13.

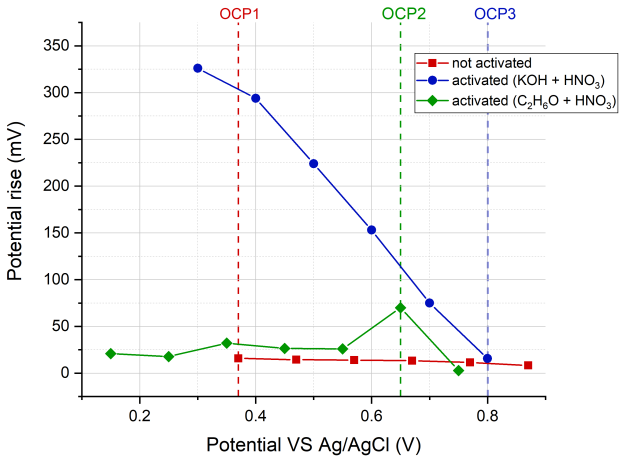

Figure 5.13: Potential rise of CNT tapes for different values of potential vs Ag/AgCl reference electrode

The activated tape with KOH and HNO_3 exhibits a remarkable behaviour for negative values of potential vs Ag/AgCl; the highest potential rise value is 326mV. In fact, since brine has more salts in higher concentrations with respect to the NaCl solution, more energy can be converted in electrical power, and so a higher potential rise was expected. For what concerns the other two samples, the result is not optimal since the observed potential rises are much lower.

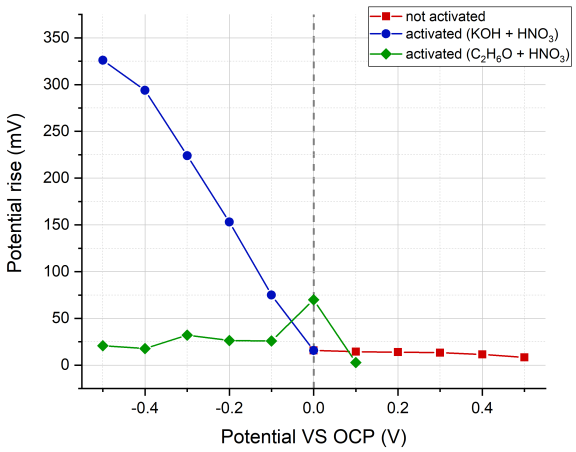

Figure 5.14: Potential rise of CNT tapes for different values of potential vs OCP

Figure 5.14 shows the same measurements but the potential applied on the electrodes is vs OCP. This can be a good indicator to see if the CNTs work better in cathodic or anodic conditions. When the tape is not activated, positive values vs OCP are applied, and a decent result is obtained. For the activated ones, it can be seen that remarkable data can be obtained when negative values vs OCP are applied. In particular, the KOH + HNO_3 activation works much better.

Chapter 6

CapMix: measurements

In this chapter, CapMix measurements are conducted using the electrodes discussed in 5. First of all, a suited cell must be designed and produced to contain the electrodes and to allow the flow of the solutions. After that, the cell is mounted with the chosen electrodes and several CapMix cycles are simulated to understand if the device is able to deliver a reasonable amount of power.

6.1 Cell design

The cell needs several features. It must have two inlets for the two solutions to enter the device and one outlet for the solution to get out. The channel must have a Y shape so one solution can easily remove the other one when inserted, avoiding stagnant points. Other two holes must be placed on the top of the cell since the two electrodes must be placed in the channel. Also, a separator has to be put between the two CNT films.
The cell is designed on SolidWorks. To simplify the manufacturing, two layers are drawn: top layer and bottom layer. In this way, all the holes and channels are dig in the bottom face of the top layer and buried cavities can be obtained when the two parts of the device are put together.

A first pen and paper design is done in order to find the exact spots for holes and channels. Then, specific dimensions are assigned to each part of the drawing. After that, the sketch is reconstructed on the CAD program.

Figures 6.1a and 6.1b show the top part of the cell. It is 40 mm long and 30 mm wide, while its height is 5 mm. There are four holes at the angles that have a diameter of 3.5 mm and are intended to host the screws that hold the two parts together. Then, three other holes with the same diameter are present: they are destined to be the inlet and the outlet of the channel. Two more openings (1 cm long and 1 mm wide) are created to let the two electrode enter the device: they

are separated by a distance of 1 cm since the electrode area is $1cm^2$. The channel connects the inlets with the outlet and has a depth of 1 mm. A sort of barrier (0.5 mm high and 0.5 mm wide) is created around the channel to improve the adhesion with the bottom part and avoid any liquid dispersion.

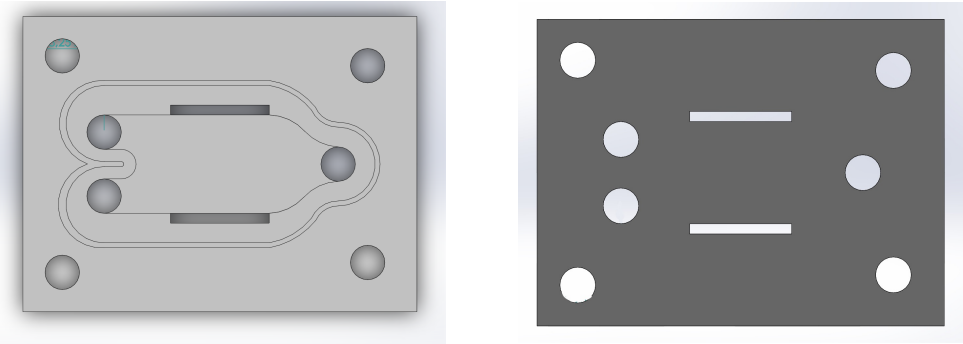

(a) Inferior plane **(b)** Superior plane

Figure 6.1: CapMix cell design - top part

The bottom part (figures 6.2a and 6.2b) is less complex. It is 40 mm long and 30 mm wide, while its height is now 3 mm; it is less thick then the other piece since less material has to be removed. There are four holes (3.5 mm diameter) on the same spots of the top half for the screws. A sort of channel (2.5 mm wide) with the same shape as the barrier in the top part is created: it will host the polymer that has to seal the two halves.

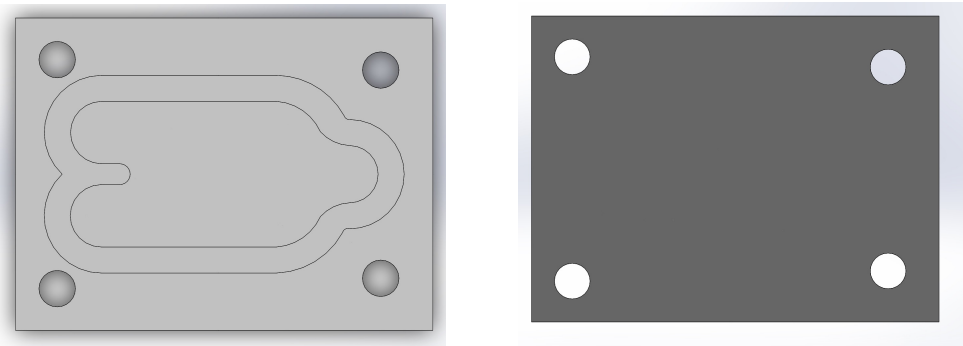

(a) Superior plane **(b)** Inferior plane

Figure 6.2: CapMix cell design - bottom part

The CAD files containing the cell design are sent to a milling machine tool. It has to replicate the same patterns to a piece of PMMA. The device utilizes different drill bits, each with different diameter depending on the shape and dimension of

the hole that must be drilled. Only the holes for the electrodes are dug with a separate tool, since the milling machine is not capable to replicate such a thin aperture. A drill with a 1 mm diameter bit is chosen to do this task.

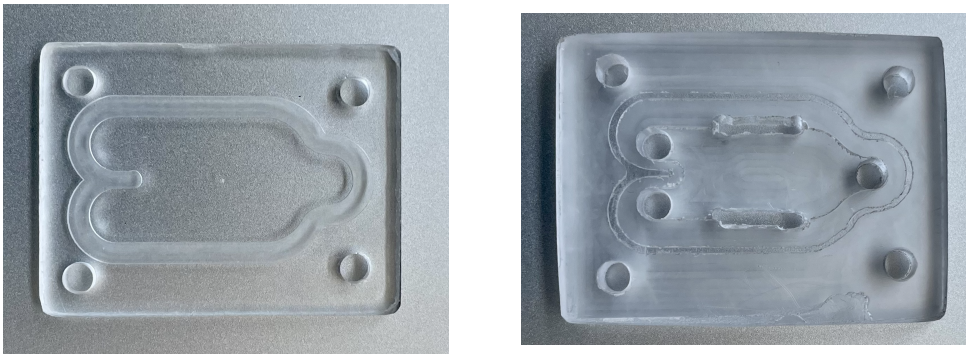

(a) Bottom part

(b) Top part

Figure 6.3: CapMix cell - final product

After these operations, the cell is polished on the edges to obtain a smooth area, especially on the corners and inside the electrodes fenditures, and PMMA residues are then removed. Figures 6.3a and 6.3b shows the ultimate result. Finally, the cell is mounted with the CNT electrodes and the separator in order to be tested (figure 6.4).

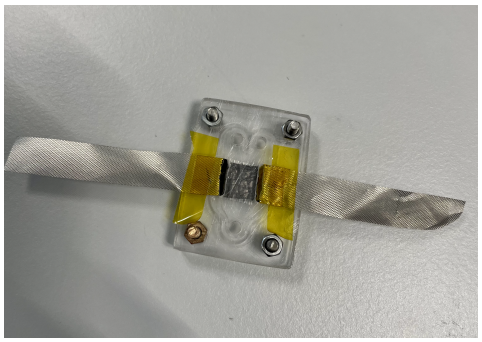

Figure 6.4: Mounted cell with electrodes and separator

6.2 CapMix Measurements

In order to simulate a realistic CapMix cycle, a suitable measurement setup must be chosen. First of all, two gear pumps are selected to allow the flow of the two solutions inside the cells; each instrument pumps the electrolyte from a batch to the inlet of the cell (figure 6.5a). Furthermore, a third gear pump is needed to prevent water leakage from the outlet of the cell (figure 6.5b); this third instrument takes the solution from the outlet and puts it in a baker.

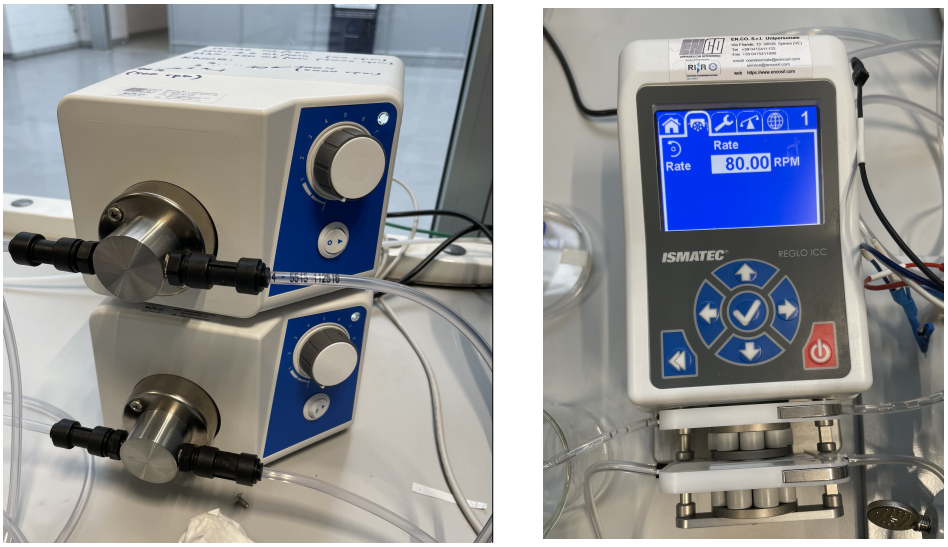

(a) **(b)**

Figure 6.5: Illustration of gear pumps used for the measurements. (a) Gear pumps for the two inlet channels. (b) Gear pump for the outlet channel.

These three pumps are connected to the cell channels and the electrodes are connected to the device that will make all the measures. In particular, the not activated tape is chosen as the negative electrode, while the tape activated with KOH and HNO_3 is chosen as the positive electrode.

6.2.1 NaCl solution

The cell is first tested with NaCl solutions as electrolytes. First of all, the high salinity solution (NaCl 0.6 M) is put inside the cell and the OCP is monitored for an hour, until its value stabilizes. After that, a procedure is set on EC Lab and the actual measurements can start.
The simulation of a CapMix cycle starts by applying a constant voltage; this method is not realistic, since normally a constant current is applied, but it is useful to

understand if a net power production is possible and to obtain the charge/discharge current values. A constant voltage equal to the OCP of the system is applied to the cell for 20 seconds; after that, the circuit is opened for 1 minute while the low salinity solution (NaCl 10 mM) replaces the high salinity one. The constant voltage is reapplied again and the circuit is opened again while salt water replaces fresh water.
In this case, after one hour the cell spontaneous potential is 400 mV. Therefore, the CapMix cycle is performed applying 400 mV as a constant voltage. Figure 6.6 shows how the voltage varies with respect to time.

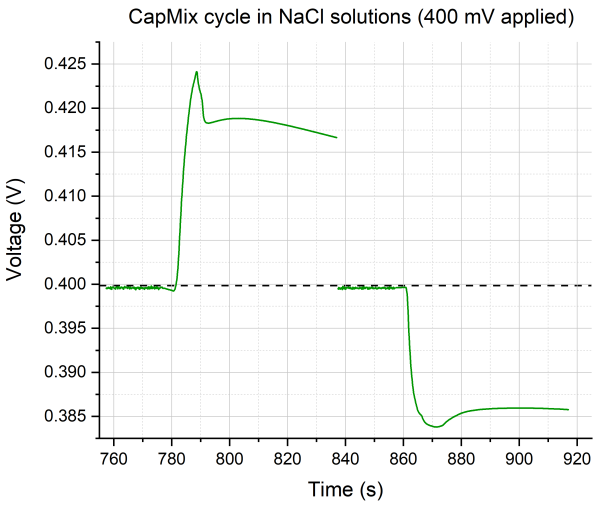

Figure 6.6: Voltage variation of a CapMix cell (NaCl solution, 400 mV applied)

The cell voltage exhibits a typical behaviour of a CapMix cycle, with a voltage rise almost equal to 20 mV. Furthermore, the charge/discharge currents are studied, to see if there is an effective power production (figure 6.8).

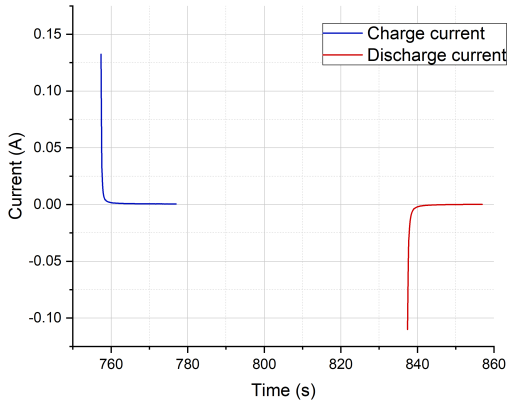

Figure 6.7: Charge/discharge currents of a CapMix cycle (400 mV applied, NaCl)

It can be observed that the discharge current (the red one) has a slightly lower peak than the charge current (the blue one); furthermore, the plateau observed for the discharge current has an absolute value higher than the charge current. This is a good indicator that the cell is producing a net power.
To simulate a more realistic process, a constant current is delivered through chronopotentiometry (CP) to the cell until its voltage reaches 400 mV both in charge and discharge steps. The current applied is 1 μA for charge and -1 μA for discharge. The cycle is shown in the following picture:

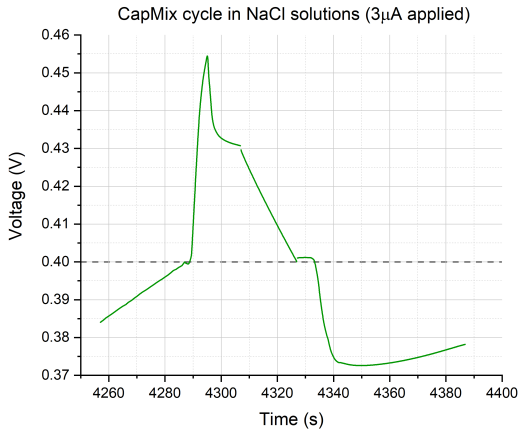

Figure 6.8: Voltage variation of a CapMix cell (3 μA applied in charge and -3 μA in discharge)

The graph is similar to the one in figure 6.6, with the difference that the voltage

applied doesn't reach 400 mV value instantly, but gradually just like in real devices. The current applied is then changed several times to get a reasonable charging/discharging time, in order to see an improvement also in power density. An optimal value in this case could be μA.

The cell capacitance is:

$$C_T = 1.25\ F/g \tag{6.1}$$

$$C_T = 20\ F/m^2 \tag{6.2}$$

The cell is able to produce an energy density equal to:

$$E_D = 51\ \mu Wh/m^2 \tag{6.3}$$

The maximum power density that we were able to obtain is:

$$P_D = 1.41\ mW/m^2 \tag{6.4}$$

6.2.2 Brine solution

After several measurements in NaCl solutions, the cell is now tested with brine solutions in two different concentrations (see tables 5.1 and 5.2). The device is filled with concentrated brine for 1 hour to let the OCP stabilize. After that, a voltage equal to the OCP is applied and the CapMix cycle is performed just like with NaCl solutions.
For the brine case, a smaller OCP than the NaCl case is expected, since the presence of bivalent salts tends to reduce the OCP of the system. However, a higher OCP is registered, around 400 mV. A first attempt is done with constant voltage at 400 mV, but with poor results. Then, the voltage applied is changed to lower values, to check if at low potentials the cell works better. The best results in terms of charge/discharge current, voltage rise and power density is obtained with a voltage applied equal to 80 mV (see figure 6.9)

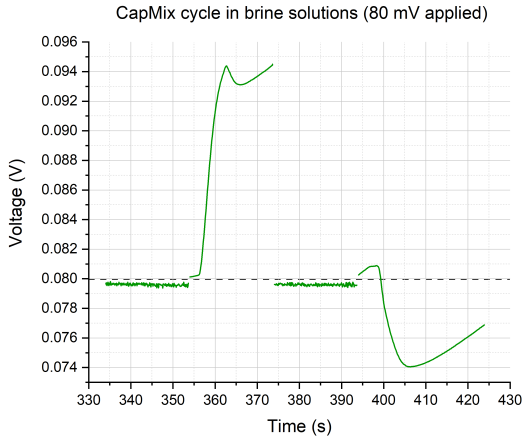

Figure 6.9: Voltage variation of a CapMix cell (brine solution, 80 mV applied)

The voltage rise observed is around 15 mV. The charge and discharge currents are reported in figure 6.10. The discharge current presents a higher peak than the charge current; both the plateaus are positive, and the discharging current plateau is smaller than the charging current one.

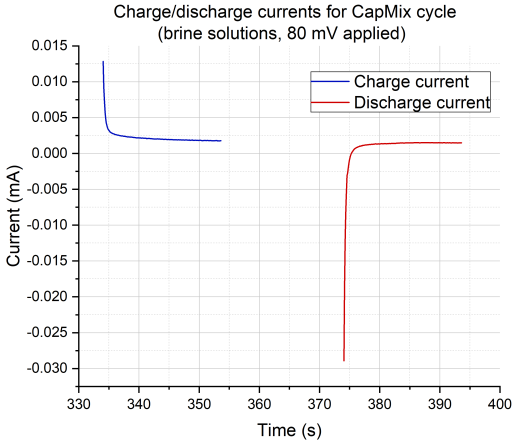

Figure 6.10: Charge/discharge currents of a CapMix cycle (80 mV applied, brine)

Some cycles with constant current are performed to try to calculate the key parameters. Several current values are applied to the cell, resulting in an optimal applied value equal to 1 μA for charging steps and $-\mu$A for discharging steps. Figure 6.11 reports thee results obtained.

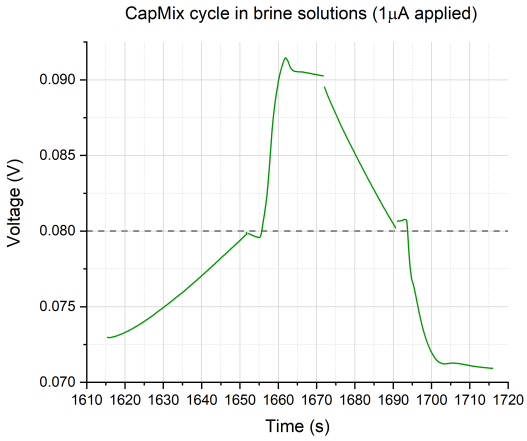

Figure 6.11: Voltage variation of a CapMix cell (1 μA applied in charge and -1 μA in discharge)

From this curve, capacitance, energy density and power density can be calculated. The cell capacitance is:

$$C_T = 1.25\ F/g \tag{6.5}$$

$$C_T = 20\ F/m^2 \tag{6.6}$$

The cell is able to produce an energy density equal to:

$$E_D = 53\ \mu Wh/m^2 \tag{6.7}$$

The maximum power density that we were able to obtain is:

$$P_D = 0.2\ mW/m^2 \tag{6.8}$$

6.3 CNT tape: before and after CapMix

In this section, an electrochemical evaluation is performed on the CNT tapes used in the CapMix measurements. This is done to check if some drops in efficiency occur after several cycles in the cell and or if the functionalization on the tape still remains during the process.
The first sample to be tested is the not activated tape. Some CVs are performed in the cathodic window and the coulombic efficiency at each potential is calculated. Figure 6.12 shows two curves superimposed: the first one refers to the cathodic analysis done to the tape before the CapMix process, while the second one refers to the sample used in the CapMix cycles in NaCl and brine solutions.

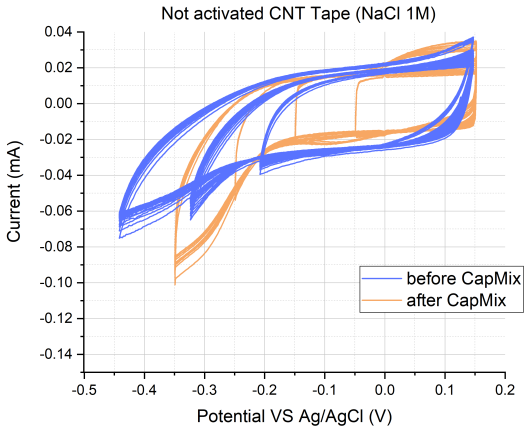

Figure 6.12: CVs in cathodic window for not activated CNT tape (before & after CapMix)

From these graphs, it is clear that the OCP is still the same for both cases, and the two shapes are very similar. From figure 6.13, it is found that the coulombic efficiency slightly drops after the process, but follows the same trend as the first tape.

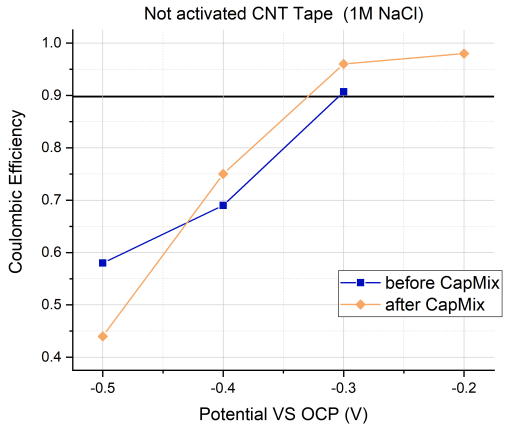

Figure 6.13: Efficiency for not activated CNT tape (before & after CapMix)

The tape activated with KOH and HNO_3 is now analysed. The CVs are taken in the anodic window and are then compared to the CVs performed before CapMix in figure 6.14. The CV shapes are similar, both indicating a good capacitive behaviour in the anodic window; the height of the CV curves is also really similar, but the OCP seems to have shifted towards higher potential values.

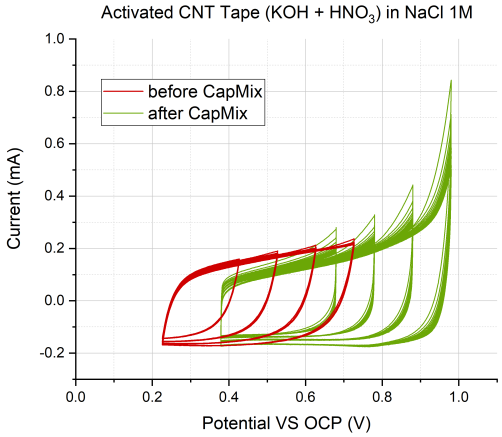

Figure 6.14: CVs in anodic window for CNT tape activated with KOH and HNO_3 (before & after CapMix)

The related efficiencies are displayed in figure 6.15. The values obtained are almost identical to the ones taken before the CapMix process. These results indicate that the functionalization done to the CNT tape is not lost during all the cycles performed with the cell. Therefore, this type of electrochemical activation can be

considered reliable for future applications.

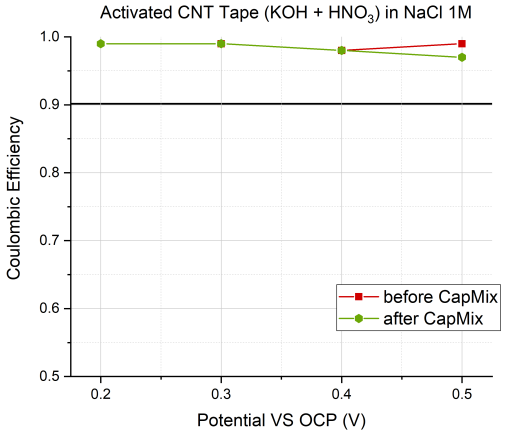

Figure 6.15: Coulombic efficiency for CNT tape activated with KOH and HNO_3 (before & after CapMix)

Chapter 7

Conclusions

Carbon nanotube tapes are carbon based materials that showed an interesting behaviour in CapMix applications. Electrochemical characterizations revealed that these tapes exhibit a quite good capacitive behaviour in salt solutions (NaCl and brine) for anodic windows, while their coulombic efficiencies were not acceptable in cathodic windows. Different electrochemical functionalizations were done to the tapes to improve efficiency and capacitance. It has been found that some of them (like KOH + HNO_3 and HNO_3 + C_2H_6O) provide a much higher efficiency both in anodic and cathodic conditions.

CapMix cycles were performed in NaCl and brine solutions. The results for the NaCl case revealed that a power production is possible with CNT tapes as electrodes. A possible suggestion for future research could be to apply different polarizations to these tapes to maximize the voltage rise of the cell and to apply various current values to minimize the time of the cycle and increase the power density achievable. For the brine case, also a net power production was found during the tests, but the power generated was lower than the previous case. It is suggested to try different combinations of new functionalized tapes and to try some polarizations to find the optimal combination for a maximum power density.

Several measurements showed that CapMix cycles with salt solutions don't consume or modify the CNT structure or electrochemical properties. In fact, coulombic efficiencies were found similar if not identical to the values calculated before any CapMix process. This characteristic could be exploited in future applications where the electrodes are subjected to much more cycles without deterioration.

Bibliography

[1] United Nations Department of Economic and Population Division Social Affairs. *World Population Prospects 2022: Summary of Results.* Tech. rep. 3. United Nations, 2022 (cit. on p. 1).

[2] Anissimov Y. Helfer F. Lemckert C. «Osmotic power with pressure retarded osmosis: theory, performance and trends — a review». In: *Journal of Membrane Science* 453 (Mar. 2014), pp. 337–358 (cit. on p. 1).

[3] Micale G. Cipollina A. *Sustainable Energy From Salinity Gradients.* Woodhead Publishing, 2016 (cit. on pp. 2, 4, 8–10, 22, 23).

[4] Gurreri L. et al. «CFD analysis of the fluid flow behavior in a reverse electrodialysis stack». In: *Desalination and Water Treatment* 48 (July 2012), pp. 390–403 (cit. on p. 2).

[5] Brogioli D. «Extracting Renewable Energy from a Salinity Difference Using a Capacitor». In: *Physical Review Letters* 103.05851 (2009) (cit. on pp. 2, 6–9, 18, 19).

[6] Childress A. E. Achilli A. «Pressure retarded osmosis: From the vision of Sidney Loeb to the first prototype installation — Review». In: *Desalination* 261 (July 2010), pp. 205–211 (cit. on p. 3).

[7] Pscheidt E. Finley W. «Hidrostatic generator». US Patent 6, 313, 545 B1 (cit. on p. 3).

[8] Zhu X. et al. «Energy Recovery from Solutions with Different Salinities Based on Swelling and Shrinking of Hydrogels». In: *Environmental Science Technology* 48 (May 2014), pp. 7157–7163 (cit. on p. 3).

[9] Isaacs J. D. Olsson M. Wick G. L. «Salinity gradient power-utilizing vapor-pressure differences.» In: *Science* 206 (Oct. 1979), pp. 452–454 (cit. on p. 3).

[10] Brogioli D. et al. «Exploiting the spontaneous potential of the electrodes used in the capacitive mixing technique for the extraction of energy from salinity difference». In: *Energy Environmental Science* 5 (Sept. 2012), p. 9870 (cit. on pp. 11–15).

[11] Pan N. Zhang S. «Supercapacitors Performance Evaluation». In: *Advanced Energy Materials* 5 (Dec. 2014), p. 1401401 (cit. on pp. 16, 29, 31–41).

[12] Baiju K. V. Paravannoor A. *Supercapacitors and Their Applications*. CRC Press, 2023 (cit. on pp. 17, 19, 20, 24, 25).

[13] Frink L. J. D. Petsev D. N. van Swol F. *Molecular Theory o f Electric Double Layers*. IOP Publishing, 2021 (cit. on p. 18).

[14] Thanh L. D. «Effective Excess Charge Density in Water Saturated Porous Media». In: *VNU Journal of Science: Mathematics – Physics* 34.4 (Nov. 2018), pp. 9–18 (cit. on p. 18).

[15] Srivastava S. K. Roy P. *Nanomaterials for Electrochemical Energy Storage Devices*. Scrivener Publishing, 2020 (cit. on pp. 21, 23–26).

[16] Ramsden J. J. «Carbon-Based Nanomaterials and Devices». In: *Nanotechnology* (Dec. 2011) (cit. on p. 26).

[17] Zhong C. et al. «A review of electrolyte materials and compositions for electrochemical supercapacitorss». In: *Chemical Society Reviews* 44.21 (Nov. 2015), pp. 7431–7920 (cit. on pp. 27, 28).

[18] Samantara A. K. Ratha S. *Supercapacitor: Instrumentation, Measurement and Performance Evaluation Techniques*. Springer, 2018 (cit. on pp. 30–34, 36, 37, 40).

[19] Wang S. et al. *Battery System Modeling*. Elsevier, 2021 (cit. on p. 41).

[20] Westphal G. et al. «Sodium Chloride». In: *Ullmann's Encyclopedia of Industrial Chemistry* (Jan. 2005) (cit. on p. 51).